Sofia University „St. Kliment Ohridski"
Faculty of Physics
Department of Meteorology and Geophysics

Abstract
Dissertation in fulfillment of the requirements for the degree “Doctor“

of
Mirna Matov

Topic:
“Climate change and projections for the 21st century in the Black Sea region and the Balkans.”

Scientific Major: Meteorology
Professional field: 4.1 Physical Sciences

Head of Department: ....
(Assoc. Prof. Dr. Gergana Gerova)

Research Supervisor : ....
(Assoc. Prof. Dr. Elisaveta Peneva)

Sofia, 2023

The dissertant is a full-time PhD student at the Department of Meteorology and Geophysics, Faculty of Physics, Sofia University "St. Kliment Ohridski" in the period February 2019 - February 2023. The thesis is 127 pages long. It consists of an Introduction and 9 chapters and a list of cited literature. Number of figures - 69. Number of tables - 14. Number of references cited - 150, including 13 websites. The dissertation was discussed and proposed for defense at an extended departmental council of the Department of Meteorology and Geophysics at the Faculty of Physics on January 26, 2023.

Sincere thanks to:

First of all, I would like to thank my supervisor Assoc. Prof. Dr. Elisaveta Peneva for her patience and the opportunity to work with her on my dissertation. For her collaboration, guidance, advice and help in the realization of the dissertation.

I would like to thank the head as. Dr. Milen Tsekov for his valuable guidance in the field of statistical analysis.

I would like to thank all my colleagues in the Department of Meteorology and Geophysics for their acceptance, assistance and encouragement.

I would like to thank the whole community of scientists working on climate whose literature I use in this dissertation.

I thank my family and all the people around me for their support and patience.

1. Relevance and aim of the thesis

The topic of climate change is one of the most debated in recent decades, as it has an impact on all aspects of human life. There is a lot of discussion about global warming, the greenhouse effect and the factors that determine them.

This is the reason why numerous research teams from different institutes are engaged in quantitative and qualitative description and prediction of climate change.

This problem is complex because it concerns the climate system: the totality of our planet's atmosphere, hydrosphere, cryosphere, lithosphere and biosphere. These components are in constant interaction with each other and any process occurring in one of them leads to changes in the others, these are so-called feedbacks. For this reason, climate change must be considered in a multidisciplinary manner and at different temporal and spatial scales. Last but not least is the human influence on climate, which has recently been considered commensurate with that of the other components of the climate system. Recent studies have found that the contribution of anthropogenic greenhouse gas emissions is responsible for at least 50% of the Earth's warming. All this makes the scientific problem of "climate change" a complex one to address.

Information on how and how much the climate will change is therefore essential. Such information can only be obtained by using sophisticated mathematical models of the interrelationships in the climate system, by knowing the factors that influence climate and how they will change. Such mathematical numerical tools are called climate models, and they make it possible to make a future projection of climate based on assumptions about the future development of society.

Global warming in the 20th century is undoubtedly the most significant change in climate. It has been accompanied by many other phenomena of varying intensity in different parts of the globe: melting of Arctic and Antarctic ice, ocean acidification, increasing droughts and flooding on land.

One of the most changing things in climate is certainly the Earth's temperature, which is undeniably increasing on average everywhere in the world. Less certain and harder to pin down are changes in the average amount of precipitation, but there is agreement that the average amount of precipitation on land in the northern hemisphere is increasing. Last but not least and one of the most interesting aspects of climate change is that the global and regional circulation is changing. However, this is not straightforward and is difficult to determine as wind is relatively difficult to determine from observations. Scientists use data from ground-based observations, aerial soundings, and climate model simulations to detect trends of changing circulation. So far, there is global agreement that the tropical zones are expanding poleward and the zone of temperate-latitude cyclones is shifting poleward accordingly. An additional difficulty is that circulation is involved in the mechanisms of climate variability and the phases of the major climate oscillations affect winds and vorticity.

The aims of the thesis can be briefly summarized as:

- To exploit the potential of the available database resulting from the implementation of the Med-Cordex project (regional numerical simulations for the present and climate projections for the 21st century) to derive and systematise expected changes in the

Balkan Peninsula-Black Sea region by selecting four climate variables: surface air temperature, precipitation, sea level pressure and surface wind speed.

- To quantify the Black Sea freeze-up phenomenon, which is a complex indicator of regional climate change. In doing so, to clarify the role of climatic factors and general atmospheric circulation, which are traditionally considered key in the region.

- To analyse future changes of the seasonal climatic centres of action Siberian maximum and Mediterranean minimum, which influence winter conditions in the region.

- To analyze future changes of extreme wind events, since the dynamical characteristics are less studied than temperature and precipitation.

High-resolution simulations of the regional climate numerical model Aladin 5.2, developed at Meteo-France, under two different scenarios defined by AR5 IPCC (2013) were used for the assessments, choosing the so-called "intermediate" and "pessimistic" scenarios for the evolution of greenhouse gas concentrations in the atmosphere in the 21st century - RCP 4.5 and RCP 8.5.

For the winter conditions in the Black Sea region, synoptic air temperature data at 2 m height from 9 coastal meteorological stations along the Black Sea coast were used - Burgas, Varna, Odessa, Kherson, Mariupol, Batumi, Trabzon, Sinop and Istanbul. The source of the data is the regular SYNOP reports distributed by the Global Surface Summary of the Day (GSOD) data archive at ncei.noaa.gov. The data cover the period from 1950 to the present, but there are many gaps, especially at the beginning of the period. The sea ice extent data is taken from the Multisensor Analysed Sea Ice Extent-Northern Hemisphere (MASIE-NH) product.

ERA-5 reanalysis data were used to estimate the intensity of the Siberian High, and CORDEX data were used for the Mediterranean Low.

2. Current state of the problem

The largest evaluations of climate change today are being made by the Intergovernmental Panel on Climate Change (IPCC), which aims to provide scientific information to governments around the world that can be used to make climate change policies. Through its assessments, the IPCC describes the extent of scientific agreement in various areas, such as the extent of changes in the climate system in the past and present, and the assessment of human influence on climate change. The IPCC has so far published six Assessment Reports, which are the most comprehensive scientific reports in the world on climate change.

In August 2021, the IPCC published the latest, sixth Assessment Report (AR6) of Working Group I, which addresses the physical basis of climate science.

Since in this thesis we evaluate 4 meteorological elements for the Balkan Peninsula and the Black Sea region - temperature, precipitation, pressure and wind, in the next few paragraphs we look at what is the real picture and what are the changes of these 4 meteorological elements on a global scale, as well as for the Balkan Peninsula and the Black Sea region, from already published studies.

2.1. Observed changes in global temperature

Temperature is one of the most certain changing weather elements. The IPCC's Fifth Assessment Report notes that since 1850, each of the last three decades on the Earth's surface has been warmer than each previous one.

Globally, surface air temperature in the first two decades of the 21st century (2001-2020) is 0.99 [0.84 to 1.10] °C warmer than in 1850-1900.9 Global surface air temperature for 2011-2020 is 1.09 [0.95 to 1.20] °C warmer than in 1850-1900, The mean values are higher over land (1.59 [1.34 to 1.83] °C) than over the ocean (0.88 [0.68 to 1.01] °C). The expected increase in global surface temperature after AR5 is mainly due to further warming, from 2003-2012 onwards (+0.19 [0.16 to 0.22] °C). In addition, methodological advances and new datasets contribute approximately 0.1 °C to the updated warming estimate in AR6 (IPCC, 2021).

It is highly likely that greenhouse gases have been the major contributor to tropospheric warming since 1979, and it is extremely likely that human-induced stratospheric ozone depletion was the major contributor to the cooling of the lower stratosphere between 1979 and the mid-1990s (IPCC, 2021).

All estimates of the change to warming in global mean temperature for 1998-2012 are within the 10th-90th percentile of the CMIP6 simulations (IPCC, 2021).

2.2. Observed changes in global precipitation

Certainty in the change in global mean precipitation is low for years before 1950 and medium for years after, due to data gaps. The incomplete global databases available show mixed and insignificant long-term trends in reported global mean precipitation changes.(IPCC.2013)

The odds are high that human influence has contributed to the observed changes in precipitation since the mid-20th century. New research on human influence on climate reinforces previous results of increases in Northern Hemisphere precipitation at mid- and high-latitudes (IPCC, 2021).

On average, with medium confidence, global land precipitation has increased since the mid-20th century, with low confidence in pre-1950 trends. Since the 1980s, there has been a more rapid increase in global land precipitation (medium confidence), with large interannual variability and regional heterogeneity. Over the global ocean, there is low confidence in estimates of precipitation trends, which is related to the uncertainty of algorithms for extracting information from satellite observations and limited in situ observations (AR6 IPCC, 2021).

2.3. Observed changes in global atmospheric pressure at sea level

Changes in pressure, however small, can lead to changes in temperature, precipitation and circulation. Van Haren et al. (2012) found a strong decrease in sea level pressure over the Mediterranean region in the winter season (January to March) for the period 1961-2000.

New ERA reanalyses show an increase in sea level pressure over the subtropics with a stronger increase during the Australian winter for the period 1979-2018. Over the Northern Hemisphere, surface pressure increases over the mid-latitude Pacific in the Northern Hemisphere winter and decreases over the mid-latitude eastern subtropical and North Atlantic in the summer, respectively. For the first half of the 20th century, inconsistencies exist in the century reanalyses as far as low-frequency changes (slow changes) are concerned (Befort et al., 2016). Overall, modern reanalysis datasets support AR5's conclusion that there is no clear signal of trends in the strength and position of the permanent and seasonal centres of pressure action since the 1950s. Instead, they highlight multi-year variations. Global sea-level pressure patterns are characterized by modes of variability (IPCC, 2021).

2.4. Observed changes in circulation over the 20th century

The strength, direction, and persistence of prevailing winds are critical to climate. Winds associated with atmospheric circulation transport heat and moisture from distant regions and thus significantly alter local climate patterns. Some winds are also given names, such as the temperate westerlies, trade winds, and equatorial windless zone, reminding us how important winds are to the climate of a region and the human societies that live in them (Reichler, 2009).

Two important examples of such changes are 1) the tropical circulation changes associated with the poleward expansion of the Hadley cells and 2) the temperate circulation changes manifested as poleward shifts of the area of strong westerly winds in temperate latitudes known as enhanced positive phase anular modes. Although both changes are associated with similar poleward shifts, it is unclear whether the two phenomena are directly related.

The meridional circulations associated with the Hadley cell are also relevant to extra-tropical circulation. For example, air moving poleward moves air toward the upper branch of the Hadley cell and tends to conserve angular momentum, turning some of the high zonal winds over the decaying branch of the Hadley cell. This is the subtropical jet stream.

One of the most significant changes seen in the meridional circulation is the poleward expansion of the Hadley and Ferrell cells.

The IPCC (2013) reports that models show the largest increase in tropical extent at 0.7° latitude per decade, for the past three decades, which is consistent with observations. However, other models simulate much smaller values, and some even negative values. When the mean meridional circulation is used as an indicator of the tropical boundary, the same simulations averaged across all models show an expansion of 0.2° latitude per decade over the period 1970-1999 (Fig. 2.1). The most recent IPCC (2021) report uses post-2013 studies against which the Hadley cell for the past 40 years has shifted poleward by about 0.1° - 0.5° per decade (Allen and Kovilakam, 2017; Davis and Birner, 2017; Grise et al., 2018; Staten et al., 2018, 2020; Studholme and Gulev, 2018; Grise and Davis, 2020). The observed expansion of the Hadley cell is primarily due to its poleward shift in the Northern Hemisphere.

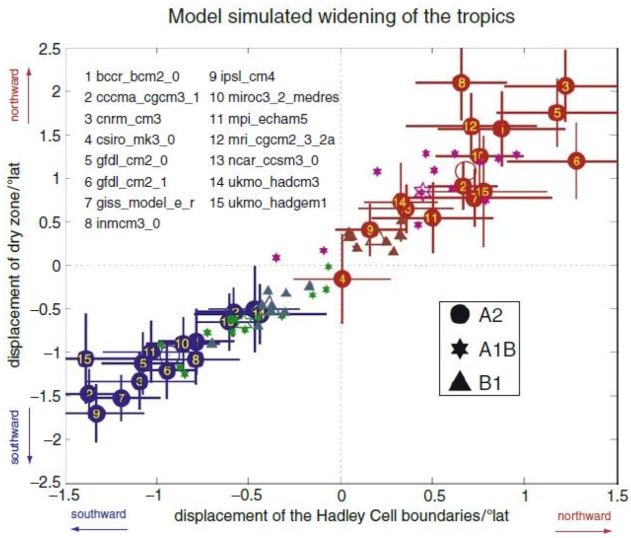

Fig. 2.1. Shift of Hadley cell boundaries to the poleward and subtropical dry zones for several climate models under 3 different climate scenarios. Red crosses refer to the northern hemisphere and blue crosses to the southern hemisphere (Lu et al., 2007).

The circulation in mid-latitudes is also undergoing important changes in relation to climate change, as shown by observations and model results. The best known examples are the so-called annular modes (AM), which are the dominant macro-scale climate oscillations in temperate latitudes (Thompson and Wallace, 2000).

Both AM have shown positive trends in both hemispheres in recent decades (Thompson et al., 2000, 2002). These are associated with lower than normal pressure over the poles, meridional shifts of cyclones and anticyclones at mid latitudes and the westerly wind zone, respectively. These trends are caused by increasing greenhouse gas emissions and decreasing stratospheric ozone (Kushner et al., 2001).

Changes in the mid-latitude circulation are largely related to trends in the tropical circulation.

2.5. Observed changes in the global surface wind

Wind over land has been measured with anemometers globally for decades, but until recently the data has rarely been used for trend analysis.

In the most recent AR6 assessment report, In situ wind datasets have been updated and quality control procedures have been improved, with particular attention to homogeneity and better preservation of true extreme values (Dunn et al., 2012, 2014, 2016).

Since the 1970s, surface winds over land have been weakening globally, which is particularly pronounced in the northern hemisphere, with low certainty. Differences between available estimates of wind speed lead to low confidence about trends in the global ocean as a whole, but most estimates show a strengthening globally over the period 1980-2000 and over the last four decades in the Southern Ocean.

The National Institute of Meteorology and Hydrology has been working quite intensively on the issue of climatic changes in the Black Sea region and the Balkan Peninsula, paying more attention to temperature and precipitation than to circulation, which is the main focus of our studies.

3. Methodology and data sources

3.1. Climate reanalyses and projections

Data on greenhouse gas emissions and concentrations are used as inputs to global climate models to calculate global climate projections. Process modelling is performed by discretizing the parameters under study within a so-called 3-D model grid and with defined time steps (at 3, 6, 12 hours, etc.) for the variables under study, which allows to integrate spatial and temporal characteristics into a single spatio-temporal model. The main limitation of global climate models is the relatively low horizontal resolution of their simulation results (over 100 km). A possible solution to the problems posed by the relatively low horizontal resolution of global models is to concentrate the modelling on a specific region of interest. However, since there are no spatial boundaries in the climate system, it is evident that the general characteristics of the climate system described by the global model must be simultaneously maintained while increasing the spatial resolution for a given region. In this thesis, results from a regional climate model based on a nested approach are used: in this approach, a regional model embedded in one of the global models (the so-called Nested Limited-Area Model, NLAM) is used. The regional model thus maintains a higher resolution for a limited area whose lateral boundaries are "nested" in the lower resolution global model. Typically, regional model simulations of climate change are run successively at increasing horizontal resolution - ~50 km, ~25 km, ~10-12 km, with the ~50 km resolution covering an area of ~5000 × ~5000 km.

The modelling of projected climate change towards future time horizons mostly takes into account changes in greenhouse gases. This is considered to be the most significant contribution of anthropogenic forcing to climate. Standardised sets of scenarios are typically used to ensure comparability of climate modelling results. The scenarios describe the possible trajectories of future human development that need to be taken into account in the input of the climate model used. The use of different scenarios in the same model produces different outputs for expected climate change. The sets of scenarios developed so far have generally been accepted by consensus by the International Science Council and have therefore been included in the climate change assessment reports published at various times by the IPCC (FAR IPCC, 1990, SAR IPCC, 1995, TAR IPCC, 2001, AR4 IPCC, 2007, AR5 IPCC, 2013).

(http://www.ipcc.ch/publications_and_data/publications_and_data_reports.shtml).

In this thesis we will work with two of the scenarios used in the IPCC Fifth Assessment Report (IPCC AR5, 2013) (http://www.ipcc.ch/report/ar5/wg1/). This set of scenarios is known as Representative Concentration Pathways (RCPs).

The RCP scenarios used in AR5 are the starting point until at least 2020 for all climate change research, as well as for the development of analyses, strategy papers and policies for adaptation and mitigation to the impacts of expected climate change in countries around the world, including the European Union. The results of the RCP4.5 and RCP8.5 scenarios are used in the thesis.

The Sixth Assessment Report uses a new set of scenarios, the so-called socio-economic scenarios (SSP) of greenhouse gas emissions, using simulations from CMIP6 (Eyring et al., 2016). The scenarios were developed based on considerations of possible socio-economic developments, the extent of action taken against climate change, and measures to control pollution in the atmosphere.

The key difference of SSP scenarios compared to RCP scenarios is the wider range of assumptions on air quality measures, and hence on short-lived gaseous air constituents that are climate forcers (Rao et al., 2017; Lund et al., 2020).

Although a new set of scenarios has been developed, AR6 uses both sets of scenarios for future climate simulations.

Numerical models estimate expected climate change as the difference between the resulting value of a climate variable for a relevant future period and its value over some historical period taken as a baseline (or reference) period. The results of so-called meteorological 'reanalysis' of historical observational data are used for comparison.

Large-scale projects comparing global climate projections evaluated by different meteorological centres and teams of scientists are, for example, the Climate Models Intercomparison Project (CMIP3) and its follow-up CMIP5 (http://cmip-pcmdi.llnl.gov/cmip5/). More than 40 global models are involved in the comparison. Similar projects comparing regional climate models are ENSEMBLE, CECILIA and CORDEX.

One of the large-scale projects is CORDEX (Coordinated Regional Climate Downscaling Experiment). It was initiated in 2009 by the World Climate Research Programme of the World Meteorological Organisation. The aim of the CORDEX project is to create a single coordinated international framework for running climate projection simulations for different parts of the world with regional models. It uses the CMIP5 archives for the RCP scenarios of the IPCC Fifth Assessment Report (IPCC AR5, 2013) and a host of new global and regional models. Regionally, the project includes sub-projects covering 13 regions of the world, two of which include the territory of Bulgaria - Region 4. Europe and Region 12. Mediterranean (Fig. 3.1).

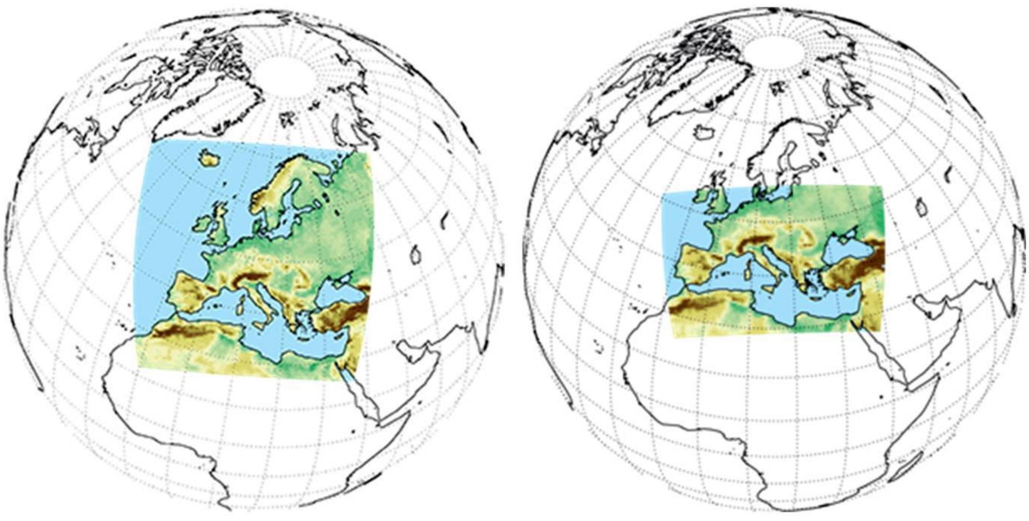

Fig. 3.1. Regions in which the territory of Bulgaria is included in Cordex

Simulations from the ALADIN 5.2 regional model are used in this thesis. ALADIN 5.2 is a local version of the French global model ARPEGE developed by CNRM, Météo-France. It uses a Lambert conformal projection and has 31 vertical levels. The model is centered at coordinates LON0=15°E, LAT0=43°E. The model is fed with a step every 6 hours by the global climate model from CMIP5 CNRM-CM5. The spatial domain of the model is 10°W, 50°E, 60°N and 25°S. All classes of greenhouse gases CO2, CH4, N2O, CFC11, CFC12 are included in the radiative scheme. The model contains six classes of aerosols - desert dust, sea salt, sulphates, carbon, organic aerosols, volcanic dust. The duration of the model set-up (spin-up) is two model years. Table 2.1 gives the main characteristics of the spatial grid of the model as well as literature sources for the sub-grid processes.

Table 2.1. Main features of the regional climate model Aladin 5.2.

ALADIN 5.2	
Institute	**Météo-France**
Grid resolution	0.11 º x0.11º
Grid (width/length)	432*288 (total grid number)
Vertical levels	31
Boundary layer scheme	Ricard and Royer 1993
Width of relaxation area	8
Convection	Mass flux, Bougeault 1985
Microphysics of clouds	Ricard and Royer 1993
Radiation exchange	Morcrette 1990
Scheme of the Earth's surface	Douville et al 2000
Main reference	Colin et al. 2010; Herrmann et al. 2011

Data for the whole Balkan Peninsula and Black Sea region were downloaded from the Med-Cordex project website http://www.medcordex.eu. The data are free, registration is required. The total data volume is ~5 GB. The results were processed and visualized with the Grid Analysis and Display System (GrADS) ver. 2.0.9a.

3.2. Observational data

In the study of winter conditions in the Black Sea region, synoptic air temperature data at 2m height were collected from 9 coastal meteorological stations along the Black Sea coast - Burgas, Varna, Odessa, Kherson, Mariupol, Batumi, Trabzon, Sinop and Istanbul. The source of the data is the regular SYNOP reports distributed by the Global Surface Summary of the Day (GSOD) data archive at ncei.noaa.gov. The data cover the period from 1950 to the present, but there are many gaps, especially at the beginning of the period.

Sea ice extent data are taken from the Multisensor Analysed Sea Ice Extent-Northern Hemisphere (MASIE-NH) product (https://nsidc.org/data/g02156). This provides daily sea ice data from 1 January 2006 to present for the Northern Hemisphere and 16 Arctic regions in polar stereographic projection (NICNSIDC, 2010).

Historical records and literature on the Black Sea ice cover and air temperature in the 20th century are taken from "The Black Sea" Volume 4 of the book series "Hydrometeorology and Hydrochemistry of the Seas of the USSR", Chapter IV.5, " Ice" (Simonov and Altman, 1991). To the best of our knowledge, this is the most comprehensive analysis of the Black Sea ice cover. Unfortunately, the data cover only the period up to 1985 and the treatment is not well documented.

We have combined meteorological maps of geopotential height of 500 hPa, sea level pressure and relative topography, with a difference between 500 and 1000 hPa in geopotential height, copied from wetter3.de. These are used to represent the synoptic conditions for several cases of intense freezing.

To qualitatively categorize how cold the winter was, we followed the approach of Simonov and Altman (1991) and Kreidin (1964): the winter severity index (WSI) is defined as the sum of the negative daily temperature values (frozen days) from December to March for each of the 9 stations. Winters are considered mild, moderate or cold using threshold values of 200 and 400 °C.

We calculated the linear trends in the graphs by fitting the data points with a linear polynomial, using the gnuplot implementation of the nonlinear least-squares Marquardt–Levenberg algorithm.

The aim of this study is to combine different sources of sea ice cover and air temperature data to investigate recent freezing and overall interannual variability over recent decades.

3.3. Statistical evaluations of model simulations for the Black Sea region and the Balkan Peninsula for modern climate (1979-2005)

In order to assess the extent to which the model simulations can be trusted for the future in the 21st century, this chapter compares the results for mean temperature, precipitation, sea level pressure and surface wind speed of numerical simulations of Aladin 5.2 and the ERA-Interim meteorological reanalysis for modern climate. Since the meteorological reanalysis has a much coarser resolution (0.75 versus 0.11°) a procedure was made to transfer the data from the coarser to the finer grid, taking into account the model topography. This was done by the model developers, who also provide the reanalysis data so processed. The period of data overlap is 1979-2005, which we refer to as the 'historical period', and for which the comparisons are made.

The statistical quantities BIAS and RMSD (Root Mean Squared Deviation) were taken as a measure of the bias of the model results from the observations:

$$BIAS = \frac{1}{N}\sum_{i=1}^{N}(X_i^m - X_i^r)$$

$$RMSD = \sqrt{\frac{1}{N}\left(\sum_{i=1}^{N}(X_i^m - X_i^r)\right)^2}$$

Where

i- the points of the model grid covering the territory of the Balkan Peninsula

N- total number of points

X_i^m – temperature, precipitation, sea level pressure or surface wind data from the Aladin model

X_i^r – temperature, precipitation, sea level pressure or surface wind data from ERA-Interim reanalysis

According to the theory of statistical analysis, BIAS indicates the tendency to underestimate or overestimate a quantity (a qualitative estimate), while RMSD estimates the absolute value of the error (a quantitative estimate).

4. Climate change in the Balkan Peninsula-Black Sea region in the present (period 1979-2005)

4.1. Comparison of temperature from model simulations and meteorological reanalysis.

4.1.1. Temperature characteristics averaged over the period

Fig 4.1 *(a)* and *(b)* show the mean surface temperature for the period 1979-2005. Fig 4.1 *(a)* showing the result from the ERA-INTERIM reanalysis and Fig 4.1 *(b)* the result from the ALADIN 5.2 model.

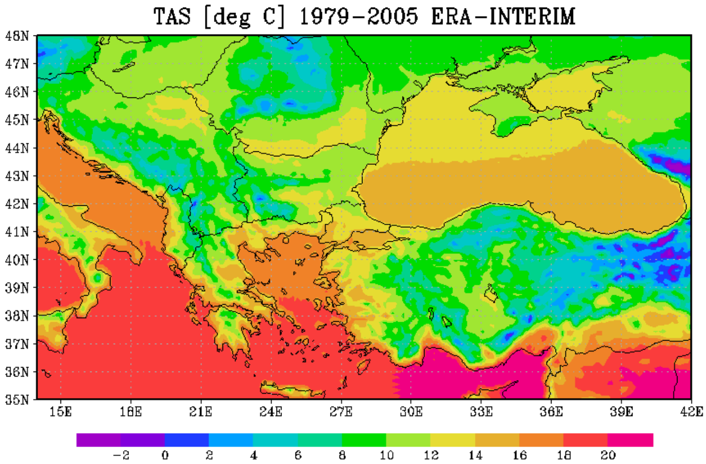

a

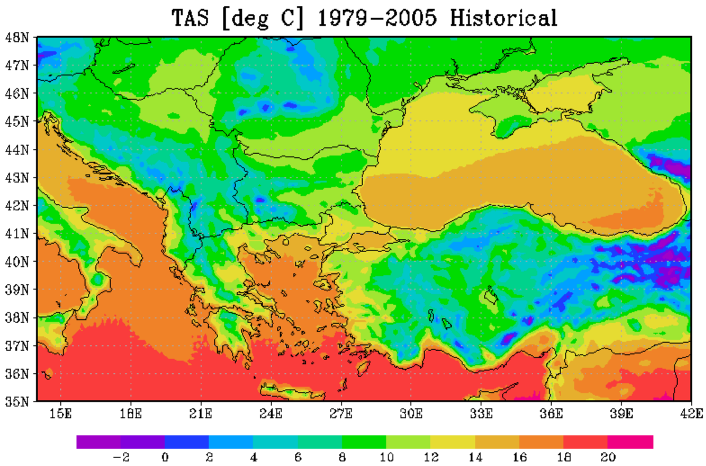

B

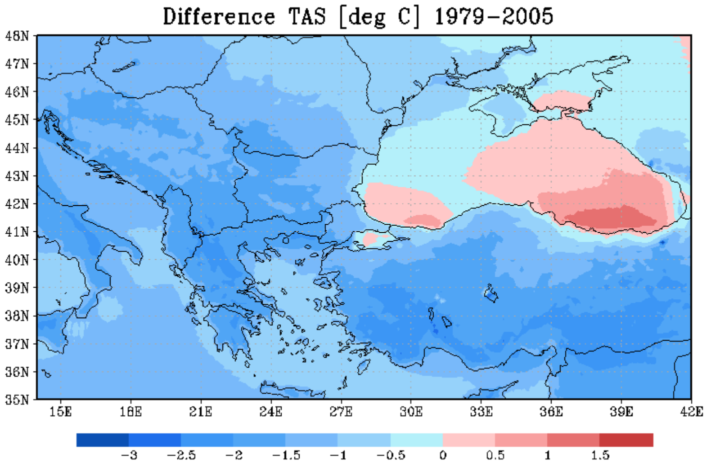

c

Fig. 4.1. Comparison between Aladin 5.2 simulations and ERA-Interim mean temperature data for 1979-2005.

In both figures, excluding the mountainous areas over land on the Balkan Peninsula, the mean temperature values range between 8°C and 14°C, with slightly more areas in Fig. 3.1 *(a)* where the mean temperature reaches values above 12°C than in Fig. 3.1 *(b)*. In Fig. 3.1*(b)*, temperatures above 12°C are seen only in the south, along the coast of Greece, while in Fig. 3.1*(b)* such areas are also seen in the more northern part of the Balkan Peninsula. This can also be seen in Fig 3.1 *(c)*, which shows the difference between Fig 3.1 *(a)* and *(b)* for the given period. Over land, the model underestimates the mean surface temperature by 2°C. A similar result is observed for the Mediterranean Sea, with mean temperature over the sea ranging between 16°C - 18°C, with the model slightly underestimating the values by about 0.5°C - 1.5°C. A different result is observed over the south-western, eastern and south-eastern Black Sea, where the model is seen to overestimate the reanalysis values by 0.5°C - 1°C in the south-western, by about 0.5°C in the eastern and by up to about 1°C - 1.5°C in the south-eastern Black Sea. Table 4.1 shows that for the whole sampled area the BIAS is negative. This analysis was also done for each season and the results are systematized in Table 4.1.

Table 4.1 shows that for the whole period and for all seasons over the whole area, BIAS is negative - the model gives lower values than the reanalysis, with the model being most accurate for winter (values most close to the reanalysis values) and least accurate for summer. The blue colour indicates that the model underestimates the reanalysis and the red colour indicates that the model overestimates the reanalysis. The brightness of the colour increases with the model uncertainty - the larger the difference to the reanalysis, the brighter the colour - bluer or redder.

Averaged surface temperature difference 1979-2005	**Temperature BIAS [ºC]**	**Temperature RMSD [ºC]**
The entire period	**-1.08**	**1.29**
Winter	**-0.69**	**1.04**

Spring	**-1.37**	**1.58**
Summer	**-1.30**	**1.86**
Autumn	**-0.97**	**1.20**

Table 4.1. BIAS and RMSD of temperature for the area of the Balkan Peninsula and the Black Sea region for the whole period 1979-2005 and by seasons.

4.1.2. Interannual variability in temperature

Having looked at the mean characteristics over the whole period, we need to address whether the model adequately represents the interannual change of mean temperature. For this purpose, the data from the model simulations and reanalysis were averaged for each year of the period considered, again focusing only on the Black Sea and Balkan Peninsula region. The result is given in Fig. 4.2.

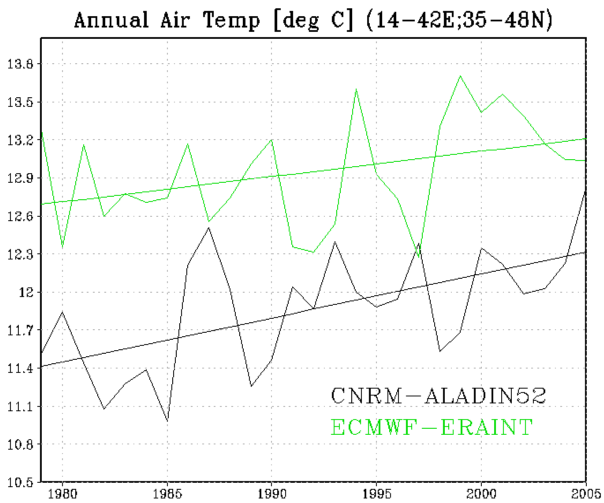

Fig. 4.2 Comparison of the interannual mean temperature trend for the Balkan Peninsula and the Black Sea from model simulations (black) and meteorological reanalysis (green). The linear trends are also given with the corresponding colours.

In Fig. 4.2, the curves from the model simulations (black) and the meteorological reanalysis (green) are not very similar. In most places they are in opposite phase, but the calculated linear trend in both cases shows an increase in mean temperature over the given period, with the model simulations showing a 0.9°C/26yr increase in mean temperature over the given period (2079-2005), and the meteorological reanalysis showing a 0.5°C/26yr increase over the same period, however the values of mean temperature from the reanalysis are slightly higher than those from the model.

4.2. Comparison of precipitation from model simulations and meteorological reanalysis.

4.2.1. Precipitation characteristics averaged over the period.

Fig 4.3 *(a)* and *(b)* shows the average precipitation for the period 1979-2005. Fig 4.3 *(a)* shows the average precipitation from the reanalysis and Fig 4.3 *(b)* shows the average precipitation from the regional climate model ALADIN 5.2.

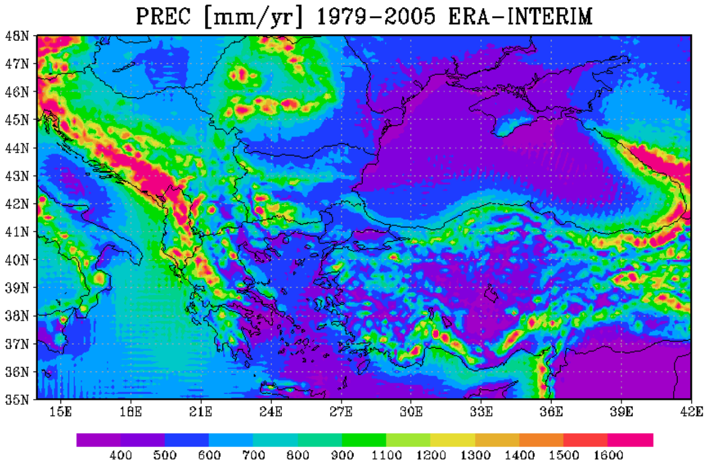

a

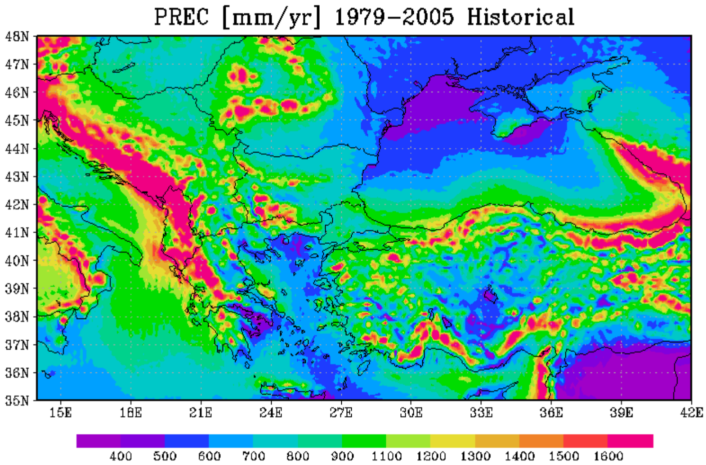

b

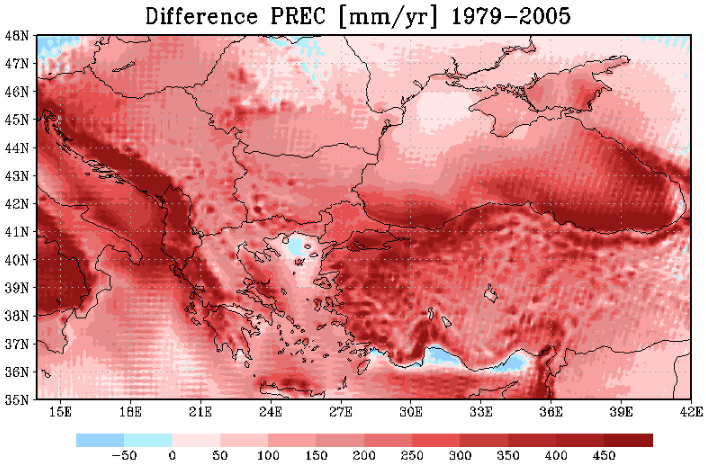

c

Fig. 4.3. Comparison between Aladin 5.2 simulations and ERA-Interim data on mean precipitation for the period 1979-2005.

On land, mountainous areas are well identified where precipitation is higher, in most places above 1500 mm/year. Outside the mountainous areas, the average precipitation on land in the Balkan Peninsula is between 600 mm/yr to about 1000 mm/yr, excluding the western part of the Balkan Peninsula where values are above 1600 mm/y due to the orthographic precipitation along the Dinar-Pindus mountain range. The model data give slightly higher values of mean precipitation, which is also seen in Fig. 4.3 *(c)* where the difference between the model data and the ERA-INTERIM data is shown. Over the Black Sea and the Mediterranean, the average precipitation is lower than over land, and again the model exceeds the values, more significantly in the southern Black Sea, by about 400 mm/yr. There are also a few areas where the model slightly underestimates the average precipitation, by about 50 mm/y, in the Mediterranean Sea off the coast of southern Turkey and in the northern Aegean Sea. Table 3.2 shows that the BIAS for the area under study is positive. This analysis was also done for each season and the results are systematized in Table 4.2.

Table 4.2 gives the BIAS and RSMD for the average precipitation over the whole period and separately for each season over the historical period. The red range indicates that the model overestimates the reanalysis. The brightness of the colour increases with the model uncertainty - the larger the difference to the reanalysis, the brighter the colour. In summer the model is most inaccurate, much more so than for the other seasons, with the uncertainty decreasing in the following order - autumn, spring, winter where the differences between the model and the renalysis are lowest. This indicates that precipitation from thermal convection is most inaccurately simulated.

Averaged precipitation difference 1979-2005	Precipitation BIAS [mm/yr]	Precipitation RMSD [mm/yr]
The entire period	**202.9**	**241.8**
Winter	**33.9**	**236.7**
Spring	**134.7**	**182.9**
Sumer	**438.3**	**544.3**
Autumn	**204.8**	**246.4**

Table 4.2. BIAS and RMSD of precipitation for the area of the Balkan Peninsula and the Black Sea region for the whole period 1979-2005 and by season.

4.2.2 Interannual variability in precipitation

Fig. 4.4 shows the inter-annual precipitation trend using the ALADIN5.2 model and the ERA-Interim reanalysis. There are years where the two curves are similar and in phase, such as 1980, 1993 and 2004, but there are also years where the curves are in opposite phase, such as 1988 and 2000. Despite the differences in the curves, the linear trend for both the model and the reanalysis is positive - increasing with time, with the trend from the model being 1.04 mm/26years and from the reanalysis 2.34 mm/26years.

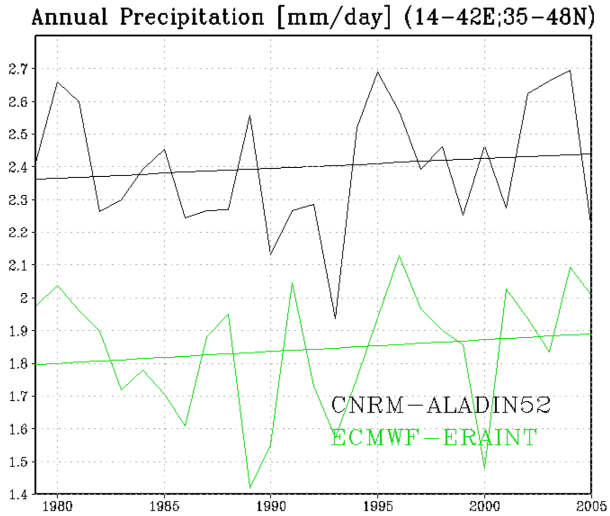

Фид. 4.4. Fig. 4.4. Comparison of the interannual change in mean precipitation for the Balkan Peninsula and the Black Sea from model simulations (black) and meteorological reanalysis (green). The linear trends are also given with the corresponding colours.

4.3. Comparison of sea level pressure from model simulations and meteorological reanalysis.

4.3.1. Sea level pressure characteristics averaged over the period.

Fig 4.5 *(a)* and *(b)* show the mean sea level pressure for the period 1979-2005. Fig 4.5 *(a)* showing the result from the ERA-INTERIM reanalysis and Fig 4.1 *(b)* the result from the ALADIN 5.2 model. Fig 4.5 *(c)* shows the difference between the model and reanalysis.

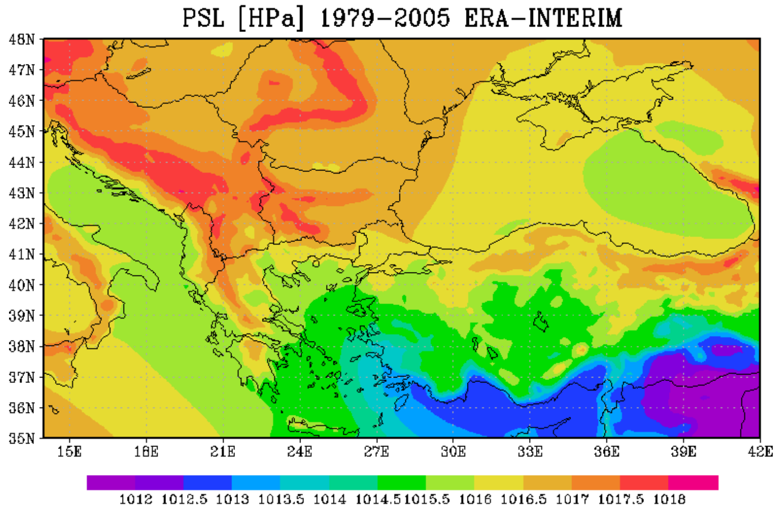
PSL [HPa] 1979-2005 ERA-INTERIM
48N
47N
46N
45N
44N
43N
42N
41N
40N
39N
38N
37N
36N
35N
15E
18E
21E
24E
27E
30E
33E
36E
39E
42E
1012 1012.5 1013 1013.5 1014 1014.5 1015.5 1016 1016.5 1017 1017.5 1018

a

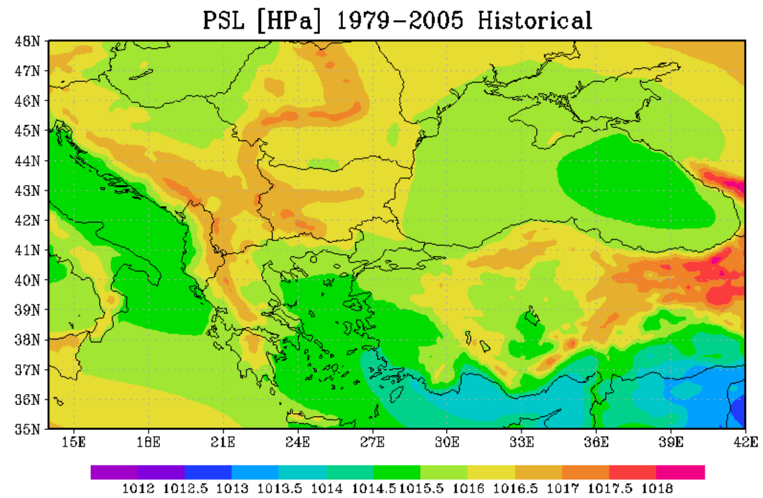
PSL [HPa] 1979-2005 Historical
48N
47N
46N
45N
44N
43N
42N
41N
40N
39N
38N
37N
36N
35N
15E
18E
21E
24E
27E
30E
33E
36E
39E
42E
1012 1012.5 1013 1013.5 1014 1014.5 1015.5 1016 1016.5 1017 1017.5 1018

B

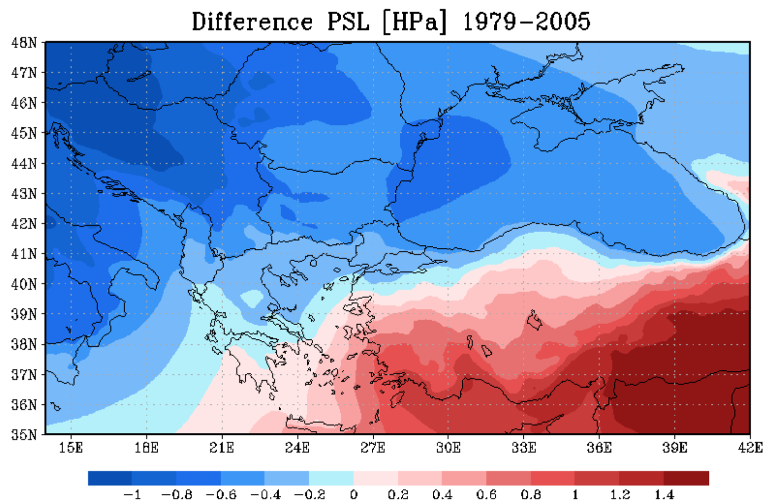
Difference PSL [HPa] 1979-2005
48N
47N
46N
45N
44N
43N
42N
41N
40N
39N
38N
37N
36N
35N
15E
18E
21E
24E
27E
30E
33E
36E
39E
42E
-1 -0.8 -0.6 -0.4 -0.2 0 0.2 0.4 0.6 0.8 1 1.2 1.4

c

Fig. 4.5 Comparison between Aladin 5.2 simulations and ERA-Interim mean sea level pressure data for the period 1979-2005.

In Fig. 4.5 *(a)*, the mean surface pressure over land in the Balkan Peninsula is between 1016.5 hPa and 1017.5 hPa. In Fig 4.5 *(b)*, for the same area, the pressure is lowered by about ½ hPa, which is well visible in Fig 4.5 *(c)*. In the southern parts of Greece the difference between the model values and the reanalysis is smaller, about 0.2 hPa. In both maps *(a)* and *(b)*, it is well seen that the pressure zonal decreases in the Mediterranean Sea, west-east direction, which occurs because of the high pressure from the Azores High in the west and the low pressure from the Asia Minor Low in the east. Fig. 4.5 *(c)* shows that in the Mediterranean Sea the model starts to overestimate the pressure, and southeastwards towards Asia Minor, the difference between model and reanalysis becomes larger, reaching 1.4 hPa. Over the western Black Sea, the mean surface pressure is about 0.5 hPa lower than the pressure over land in the Balkan Peninsula. In the eastern part of the sea the pressure is lower by about 1 hPa. Fig. 4.5 *(c)* shows that the model underestimates the values of the mean surface pressure, with a difference of about 0.8 hPa in the western part of the sea and about 0.4 hPa in the eastern part. This analysis was also done for each season and the results are systematized in Table 4.3.

Table 4.3 gives the BIAS and RMSD of the averaged sea level pressure. The red colour indicates that the model overestimates reanalysis, which is only observed in winter, and the blue colour indicates that the model underestimates reanalysis, which is observed in all other seasons as well as for the whole period. The brightness of the colour increases with the model uncertainty - the larger the difference to the reanalysis, the brighter the colour. Accordingly, we see that for summer and autumn the model is most accurate, with BIAS being negative. The bias is slightly larger in winter, where BIAS is positive, and we see that for spring the difference is largest relative to the reanalysis, with BIAS again negative.

Averaged sea level pressure difference for the period 1979-2005.	Sea level pressure BIAS [hPa]	Sea level pressure RMSD [hPa]
The entire period	**-0.10**	**0.73**
Winter	**0.90**	**1.56**
Spring	**-0.87**	**0.98**
Summer	**-0.20**	**0.75**
Autumn	**-0.23**	**0.67**

Table 4.3 BIAS and RMSD of sea level pressure for the area of the Balkan Peninsula and the Black Sea for the whole period 1979-2005 and by all seasons.

4.3.2. Interannual variability in sea level pressure.

Fig 4.6 shows the interannual trend of surface atmospheric pressure over the whole period. It can be seen that the two curves are quite similar and almost everywhere in phase, except for 1993 and 2003. In 1998 the curves match perfectly. The strange thing is that the linear trend in the reanalysis is constant, while in the model the trend decreases by about 0.2hPa/26 yr.

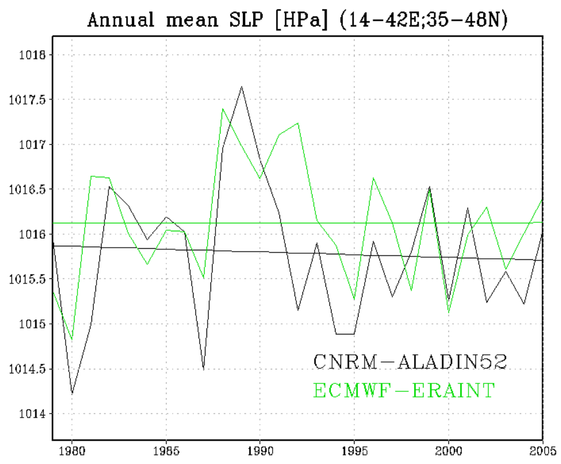

Fig. 4.6. Comparison of the interannual trend of mean sea level pressure for the Balkan Peninsula and the Black Sea from model simulations (black) and meteorological reanalysis (green). The linear trends are also given with the corresponding colours.

4.4. Comparison of surface wind speed from model simulations and meteorological reanalysis.

4.4.1. Surface wind characteristics averaged over the period.

Fig 4.7 shows the averaged wind speed over the period 1979-2005 from the Aladin 5.2 model simulations *(a)*, the ERA-Interim reanalysis *(b)* and the model minus reanalysis difference *(c)*.

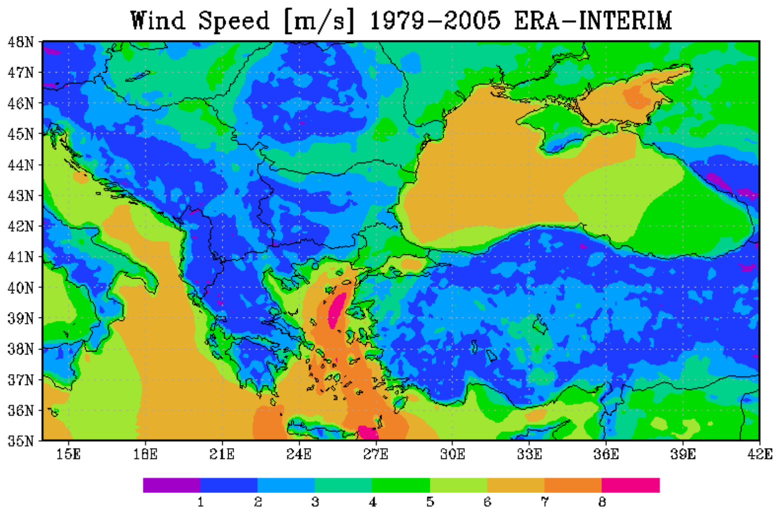

a

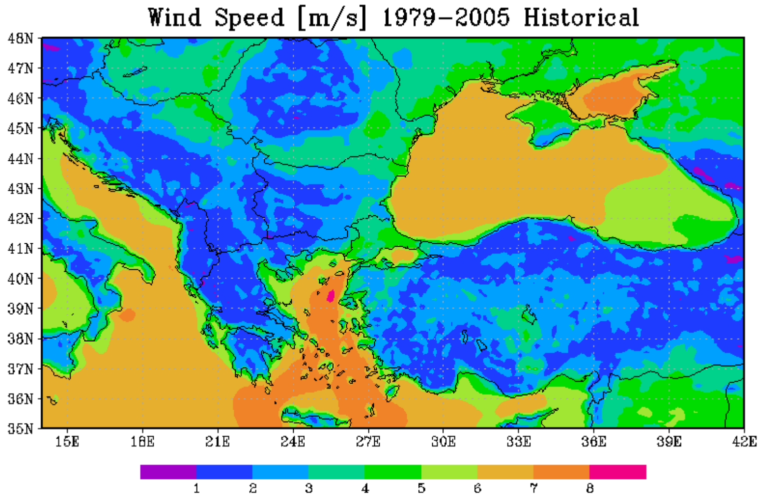

b

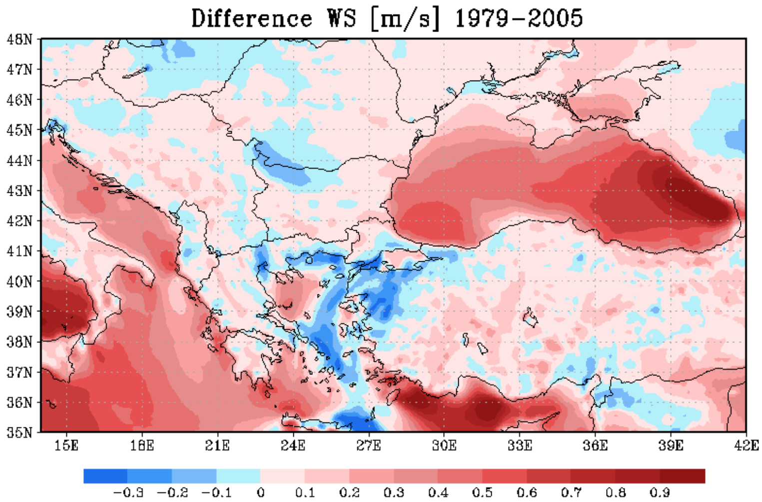

c

Fig. 4.7. Comparison between Aladin 5.2 simulations and ERA Interim surface wind data for the period 1979-2005.

There is a good similarity between Fig. 4.7 *(a)* and Fig. 4.7 *(b)* - both the model and the reanalysis give similar values of the mean surface wind speed for the land on the Balkan Peninsula - between 1 m/s and 3 m/s, which is also visible in Fig. 4.7 *(c)* - the difference between the model and the reanalysis is very small, ±0.1 m/s. The mean wind speed over the seas is higher than that on land, about 6 m/s -7 m/s, with an area in the northern Aegean with a mean wind speed of about 8 m/s. In the western Black Sea, the average surface wind speed is lower, 4 m/s -5 m/s. Over the water basins the difference between model and reanalysis is slightly larger than that on land. Over the Black Sea, the model overestimates the reanalysis values by about 0.4 m/s over most of the sea, with the speed increasing in the eastern part to 0.9 m/s. In the northern and eastern Aegean, the model underestimates the mean surface wind speed by about 0.2 m/s - 0.3 m/s, as well as in the Mediterranean east of Crete. In the rest of the Mediterranean, the model again overestimates the reanalysis values, with the largest difference observed off the southwestern Turkish coast. For the whole sampled area, the calculated BIAS is positive, as seen in Table 3.4. This analysis was also done for each season and the results are systematized in Table 4.3.

Table 4.4 provides the BIAS and RMSD for the entire period as well as for each season. The red range indicates that the model overestimates the reanalysis, and the brightness of the colour increases with the model uncertainty - the larger the difference, the brighter the colour. Accordingly, we see that for summer and autumn the model is most accurate, with the bias increasing for winter and especially spring. It can be seen that for the whole period the bias is between the winter values and the summer values.

Averaged surface wind speed difference for the period 1979-2005	Wind speed BIAS [m/s]	Wind speed RMSD [m/s]
The entire period	**0.17**	**0.29**
Winter	**0.21**	**0.37**
Spring	**0.36**	**0.47**
Summer	**0.04**	**0.35**
Autumn	**0.05**	**0.24**

Table 4.4 BIAS and RMSD of surface wind for the area of the Balkan Peninsula for the whole period 1979-2005, and for each season.

4.4.2. Interannual variability in surface wind speed

Fig 4.8 shows the inter-annual trend of the mean surface wind speed. The curves do not overlap much. The most similarity is observed in the year 2000. After 2000 the curves are in phase. The linear trend from both the model and the reanalysis shows a slight decrease in the mean surface wind speed for the period 1979-2005, with 0.04 m/s/26yr for the model and 0.01 m/s/26yr for the reanalysis.

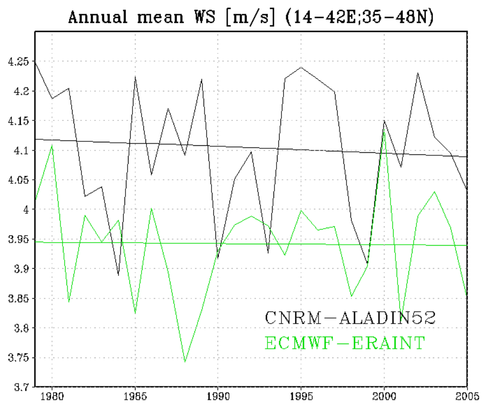

Fig. 4.8. Comparison of interannual surface wind for the Balkan Peninsula and the Black Sea from model simulations (black) and meteorological reanalysis (green). The linear trends are also given with the corresponding colours.

5. Climate projection in the Balkan Peninsula-Black Sea region by the end of the 21st century

Based on the resulting estimates of the ability of the Aladin 5.2 model to simulate climate in the Black Sea and Balkan Peninsula region, we will draw some conclusions about future climate changes that can be expected in the 21st century. This chapter presents the results obtained from the climate simulations under the two scenarios used: RCP4.5 and RCP8.5. The present century is divided into three 30-year periods: 2011-2040, 2041-2070 and 2071-2100.

The results obtained for the expected climate changes refer to the mean values of temperature at 2 m height, precipitation, surface pressure and surface wind based on their averaged values for the defined periods and for the respective scenarios, relative to the historical period 1979-2005.

5.1. Expected changes in temperature

5.1.1 Expected changes in temperature at 2 m height for the periods 2011-2040, 2041-2070 and 2071-2100.

Fig. 5.1 shows maps of the differences in mean temperature from the historical period for the RCP 4.5 scenario *(a,c,e)* and the RCP 8.5 scenario *(b,d,f)* for the three future periods - *(a)* and *(b)* for the period 2011-2041, *(c)* and *(d)* for the period 2041-2070 and *(e)* and *(f)* for the period 2071-2100.

In both scenarios, for all time periods, average temperatures are expected to increase, which is logical with the trend of global warming.

For the first future period under the RCP4.5 scenario, the temperature is expected to increase by about 1°C in the Balkan Peninsula and by about 1.1°C in Asia Minor, while for the RCP8.5 scenario for the same regions the increase is about 1.1°C for the Balkan Peninsula and about 1.2°C for Asia Minor, respectively. Over most of the sea basins, the increase in mean temperature is expected to occur slightly slower than that over land. For the Mediterranean Sea, under the RCP4.5 scenario, the model shows that the temperature should increase by about 0.8°C-0.9°C, while under RCP8.5 it should increase by about 1°C. A strange picture emerges for the Black Sea, where the RCP4.5 scenario gives slightly higher values for mean temperature over the sea than RCP8.5, 0.9°C - 1°C and 0.8°C respectively.

For the period 2041-2070, the difference between the two scenarios *(c)* and *(d)* is much more significant than for the first period 2011-2040. Under RCP4.5, in the southern Balkan Peninsula and Adriatic Sea the increase is expected to be about 1.6°C, in the Mediterranean Sea about 1.2°C, in the northern Balkan Peninsula, Asia Minor and the Black Sea the model predicts a temperature increase of about 1.8°C. In the northern Black Sea and Asia Minor, it reaches 2°C. The largest increase is observed in the Azov Sea area and the northern Black Sea coast by about 2.2°C. For the pessimistic scenario the differences are even higher. For the whole Balkan Peninsula and Asia Minor, the difference to the historical period is 2°C - 2.4°C. Over the Mediterranean under RCP8.5, the mean temperature is expected to increase by about 1.8°C - 2°C, and in the Adriatic and eastern Black Sea by about 2°C - 2.2°C. In the western Black Sea, the difference increases and reaches about 2.4°C, and up to 2.6°C in the north. In the Sea of Azov, simulations show that the pessimistic scenario temperature is expected to increase by about 2.6°C.

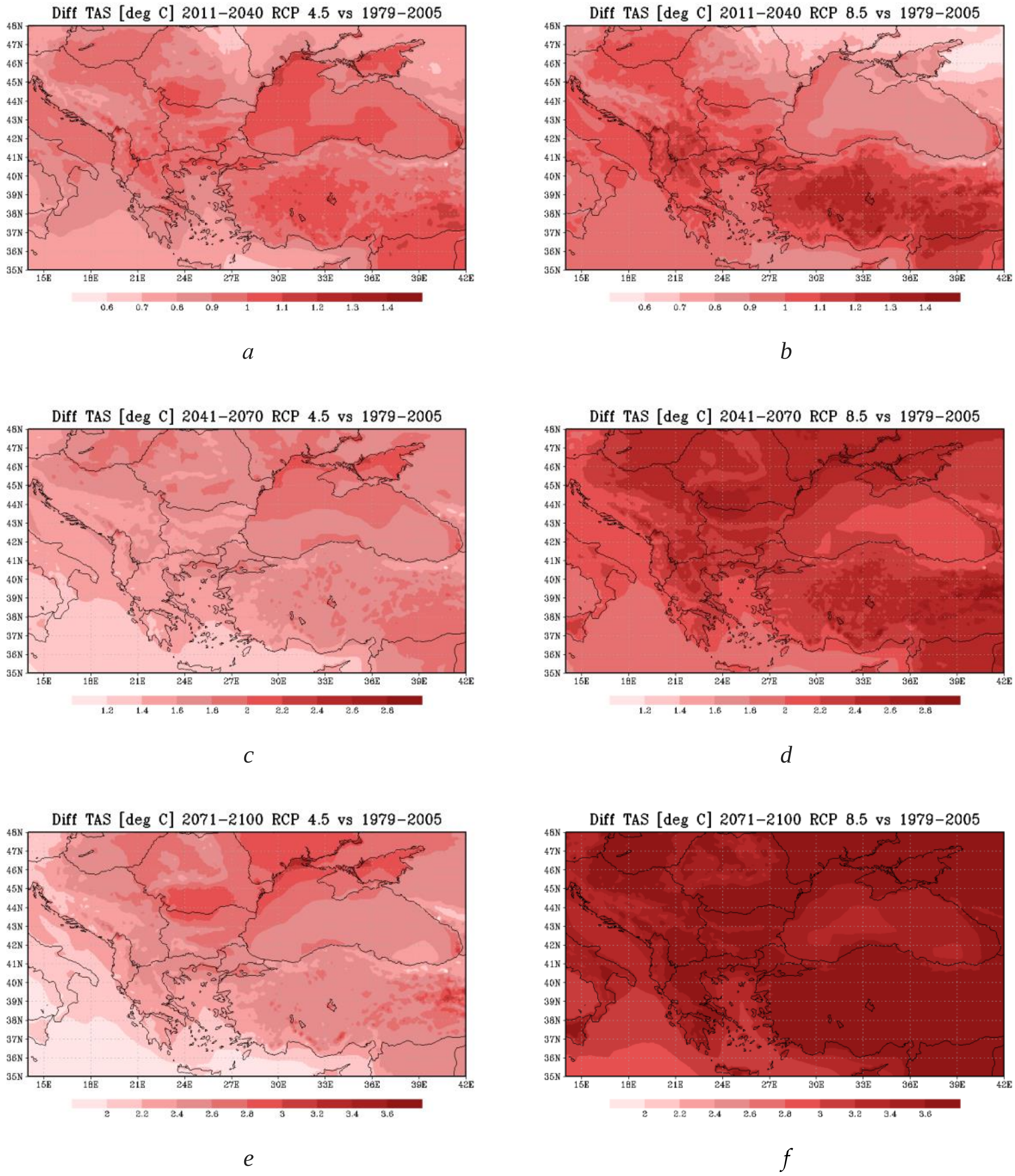

Fig. 5.1. Comparison of mean temperature under RCP 4.5 and RCP 8.5 scenarios for the period 2011-2040 (a,b), 2041-2070 (c,d) and 2071-2100 (e,f) and the historical period 1979-2005.

For the last period *(e)* and *(f)*, the differences are most significant, both between the two scenarios and relative to the historical period. Under RCP4.5, the mean temperature is expected to increase by about 2.4°C-2.6°C in the Balkan Peninsula and the Black Sea, and above 3°C in the northern Black Sea. Over the Mediterranean, the increase in mean temperature is expected to be around 2°C. For scenario RCP8.5, Fig. 4.3 *(e)* shows that almost everywhere the temperature is expected to increase by more than 3°C, with most places exceeding 3.6°C. Such an increase in temperature would affect a huge number of things - for example, one of these things is the ecosystem - many plants and animals would decline drastically and some would become extinct. It is also likely to lead to water shortages in large cities, droughts in some places, floods in others.

Table 5.1 provides the BIAS and RMSD for each of the three periods under both scenarios relative to the historical period. The red colour indicates that the simulations show an increase in temperature for all three future periods. The brighter the colour, the greater the difference relative to the present period. The table shows well that for each scenery, each future period is expected to be warmer relative to the present climate, with larger differences for RCP8.5.

Difference from the historical period 1979-2005	Temperature BIAS [^{0}C]	Temperature RMSD [^{0}C]
RCP 4.5 2011-2040	0.90	0.91
RCP 4.5 2041-2070	1.64	1.65
RCP 4.5 2071-2100	2.42	2.43
RCP 8.5 2011-2040	0.96	0.98
RCP 8.5 2041-2070	2.27	2.28
RCP 8.5 2071-2100	3.65	3.67

Table 5.1. Values of the mean and standard deviation of the model results for temperature under the two scenarios RCP 4.5 and 8.5 and the three future periods, in the 21st century, averaged over an area covering the Balkan Peninsula and the Black Sea.

5.1.2 . Interannual variability of average temperature for RCP4.5 and RCP8.5 scenarios 2011-2100.

Figure 5.2 shows the interannual temperature variability for the entire future period 2011-2100 - RCP4.5 (red) and RCP8.5 (blue) scenarios. Although the two curves do not overlap in many places, it is clearly visible that the trends for both scenarios increase over time, with the simulations showing that warming would occur much more rapidly under RCP8.5. The linear trend for RCP4.5 is 1.8°C /90year, which is 0.2°C /10year. Under this slightly more optimistic scenario, the average temperature in 2100 is expected to be about 14.2°C. The linear trend for RCP8.5 is estimated to be 4°C/90 yr, which is 0.4°C/10 yr. This means that by 2100, according to the simulations, the average temperature under this scenario would reach a value of 16.2°C, which is 2°C higher than under RCP4.5.

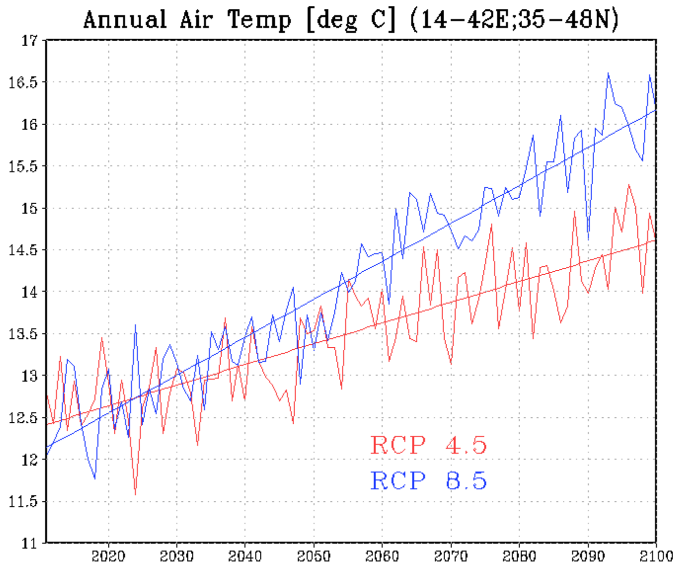

Fig. 5.2. Comparison of the interannual mean temperature variability for the Balkan Peninsula and the Black Sea in model simulations for the RCP 4.5 scenario (red) and the RCP 8.5 scenario (blue) for the period 2011-2100.

5.2. Expected changes in average precipitation

5.2.1 Expected changes in average precipitation for the periods 2011-2040, 2041-2070 and 2071-2100.

Fig. 5.3 shows maps of the differences compared to the historical period and under the RCP 4.5 *(a,c,e)* and RCP 8.5 *(b,d,f)* scenarios for average precipitation for the three future periods - *(a)* and *(b)* for the period 2011-2041, *(c)* and *(d)* for the period 2041-2070 and *(e)* and *(f)* for the period 2071-2100.

It is much more difficult to make a projection for precipitation than for temperature, as it is more difficult to determine the change in average precipitation in the past because of the lack of sufficient data (IPCC, 2021).

The first row of Fig 5.3 *(a)* and *(b)* shows the differences for the period 2011-2040 under the two scenarios compared to the historical period. The pictures are quite similar. Interestingly, under RCP4.5 a few areas stand out where the model simulations show that precipitation will increase for the first future period - in the western Aegean by about 180 mm/yr and in the western Black Sea by about 120 mm/yr, while under RCP8.5 for these areas a slightly smaller change in precipitation is expected compared to the historical period - between 60-90 mm/yr. In the western part of the Balkan Peninsula above the Dinaric Alps, both scenarios expect a decrease in average precipitation of about 90 mm/yr. In the eastern part of the Balkan Peninsula under RCP4.5 slightly higher values of average precipitation are expected, with about 30-60 mm/y, while for RCP8.5 there are areas where a slight increase is expected, with about 30 mm/y, but also areas with a slight decrease in average precipitation, with about 30 mm/y. Over the Mediterranean Sea, both scenarios expect an increase in precipitation of about 90 mm/yr, with values again slightly higher in scenario RCP4.5.

Interestingly, over Turkey, both scenarios show a decrease in average precipitation of about 30-60 mm/yr. Over the Black Sea, both scenarios expect an increase in average precipitation (more in the western part), with a slightly higher increase under RCP4.5. RCP8.5 shows an area in the eastern part of the sea where average precipitation is expected to slightly decrease.

For the second period *(c)* and *(d)*, over all seas covered by the sampled region, an increase in average precipitation is expected in both scenarios, with about 60-90 mm/yr in the western Black Sea and over 120 mm/yr in the northwestern Aegean Sea. Over the whole Balkan Peninsula, the same increase in average precipitation is expected under both scenarios (more under RCP4.5), with the exception of the Dinaric Alps where a drought is expected compared to the historical period. Over Turkey, drought is expected in the results of both scenarios relative to the base period, probably due to the expansion of the subtropical zones to the north.

For the latter period *(e)* and *(f)*, in both scenarios, in the same areas, precipitation is expected to increase, and in the same areas, to recede, but in scenario RCP8.5 both the drought and the increase in precipitation is more intense.

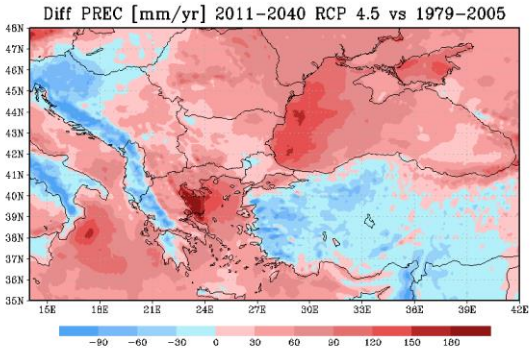

a

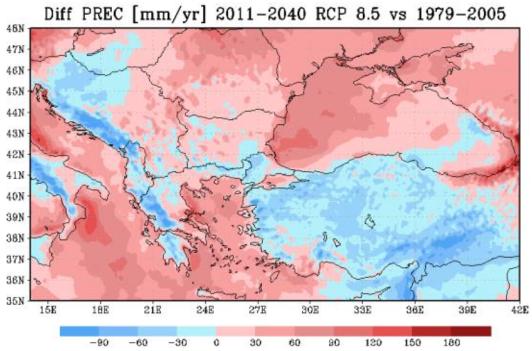

B

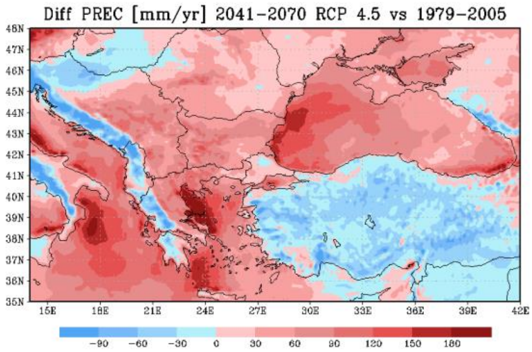

c

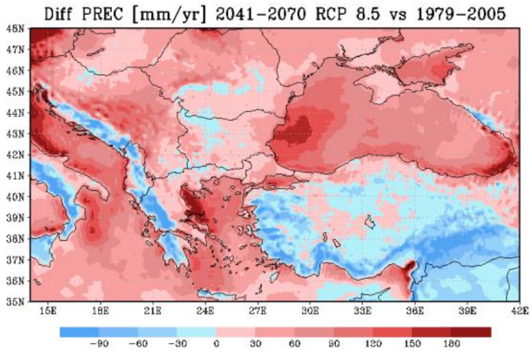

d

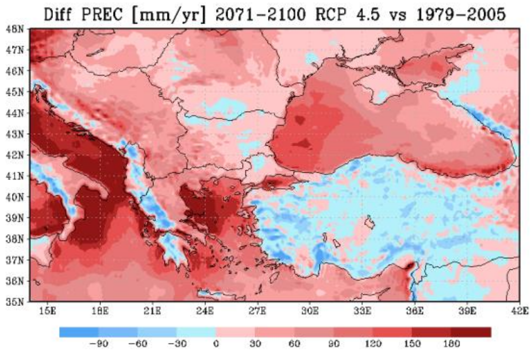

e

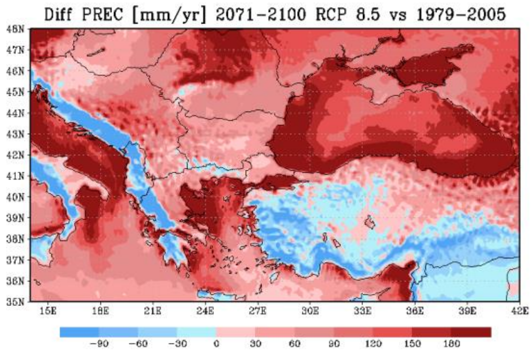

f

Fig. 5.3. Comparison of of mean precipitation under RCP 4.5 and RCP 8.5 scenarios for the period 2011-2040 (a,b), 2041-2070 (c,d) and 2071-2100 (e,f) and the historical period 1979-2005.

Table 5.2 provides the BIAS and RMSD for each of the three periods under both scenarios relative to the historical period. The red colour indicates that an increase in average precipitation is expected and the brightness indicates the intensity - the redder the colour, the greater the expectation of an increase in average precipitation. As can be seen in both scenarios, for each following period the increase is expected to be greater compared to the previous period. For the first period, the average values are higher under the RCP4.5 scenario, for the second the increase per year is almost the same for both scenarios, and for the third period, the increase is much larger under RCP8.5.

Difference from the historical period 1979-2005	Precipitation BIAS [mm/yr]	Precipitation RMSD [mm/yr]
RCP 4.5 2011-2040	30.9	58.5
RCP 4.5 2041-2070	34.8	69.6
RCP 4.5 2071-2100	52.7	83.7
RCP 8.5 2011-2040	17.5	47.8
RCP 8.5 2041-2070	35.3	68.3
RCP 8.5 2071-2100	79.7	128.8

Table 5.2. Values of the mean and standard deviation of the model results for precipitation under the two scenarios RCP 4.5 and 8.5 and the three future periods, in the 21st century, averaged over an area covering the Balkan Peninsula and the Black Sea.

5.2.2 Interannual variability of average precipitation under the two scenarios for the period 2011-2100.

Figure 5.4 shows the inter-annual trend of the average precipitation for the entire future period 2011-2100 under the RCP4.5 (red) and RCP8.5 (blue) scenarios. It can be seen that the two curves are not very similar and the two scenarios for one year may give quite different results, but if we look at the linear trend, it is well seen that over time the average precipitation increases under both scenarios. What is interesting here is that by 2041, the average precipitation is higher under the RCP4.5 scenario, not because it is increasing faster, but because from the very beginning of the graph, the average precipitation is higher under the RCP4.5 scenario. From 2011-2041, the RCP8.5 scenario average precipitation value is lower than the RCP4.5 scenario, but increases faster over time than the RCP4.5 scenario, catching up to the RCP4.5 average around 2041, and continuing to increase faster than the RCP4.5 forward in time. For the first 30 years to 1941, the linear trend under RCP4.5 is 0.04 mm/day and under RCP8.5 0.07 mm/day. For the entire period, the linear trend under RCP4.5 is 0.1 mm/day and under RCP8.5 0.2 mm/day.

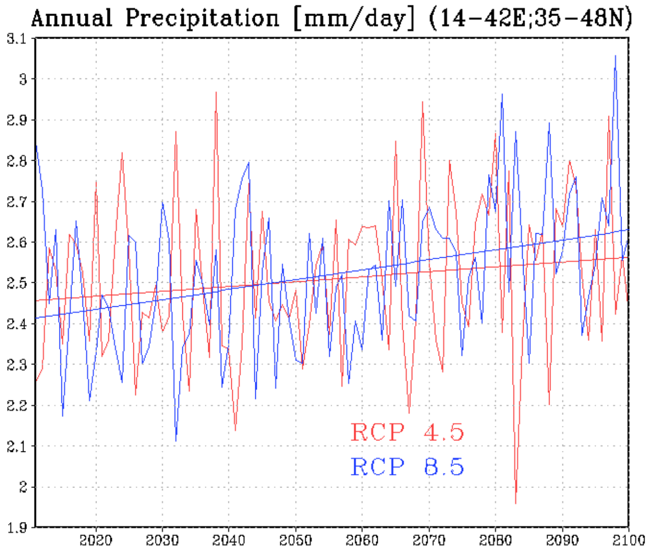

Fig. 5.4. Comparison of the interannual mean precipitation variability for the Balkan Peninsula and the Black Sea in model simulations for the RCP 4.5 scenario (red) and the RCP 8.5 scenario (blue) for the period 2011-2100.

5.3. Expected changes in sea level pressure

5.3.1. Expacted changes in sea level pressure under the two scenarios for the periods 2011-2040, 2041-2070 and 2071-2100.

Fig. 5.5 shows maps of the differences compared to the historical period and under the RCP 4.5 *(a,c,e)* and RCP 8.5 *(b,d,f)* scenarios for average p sea level pressure for the three future periods - *(a)* and *(b)* for the period 2011-2041, *(c)* and *(d)* for the period 2041-2070 and *(e)* and *(f)* for the period 2071-2100.

Figure 5.5 *(a)* and *(b)* show the differences under the two scenarios relative to the historical period 2011-2040. The differences are small. The RCP4.5 scenario shows a slight strengthening of the Asia Minor depression, by about 0.1 hPa. Over the Black Sea and the Mediterranean Sea, a slight increase in sea level pressure is observed - about 0.1 hPa - 0.2 hPa, over Greece and eastern Bulgaria the increase is about 0.3 hPa, in western Bulgaria and, Romania, Serbia it is about 0.4 hPa, reaching also up to 0.5 hPa in the northwest, which leads us to think that the Icelandic minimum, which has an influence over the whole of Europe, is expected to weaken. Under the RCP8.5 scenario, mean surface pressure is expected to increase more than under the RCP4.5 scenario. Over the Black Sea by about 0.4hPa to the south and

0.5hPa to the north. Over the southern parts of the Balkan Peninsula by about 0.5 hPa. Over mountainous regions in Bulgaria and northwards towards central and western Europe, mean sea level pressure is expected to increase by more than 0.6 hPa under scenario RCP8.5.

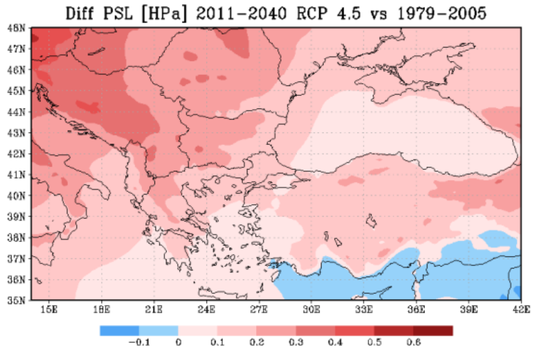

a

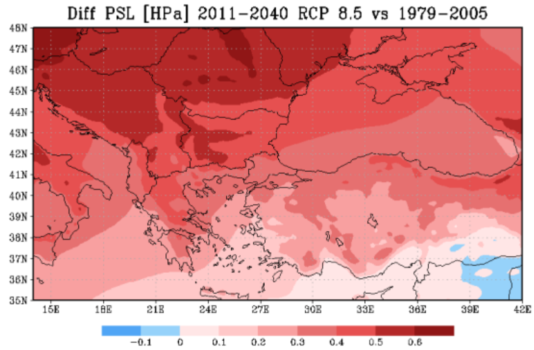

B

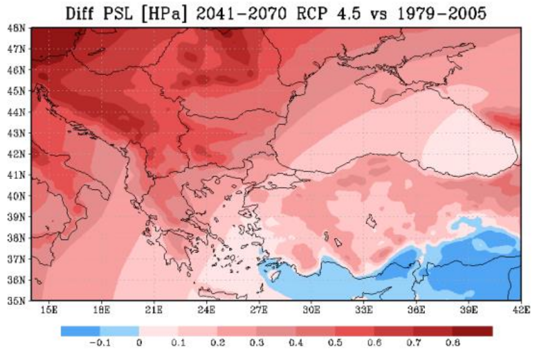

c

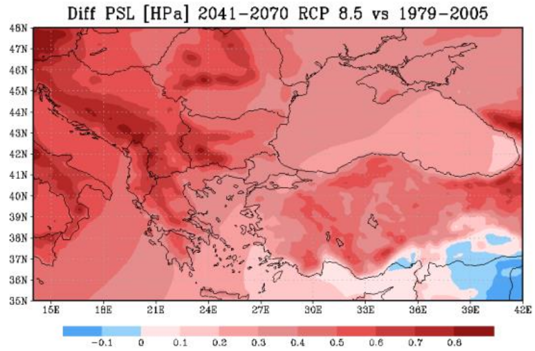

D

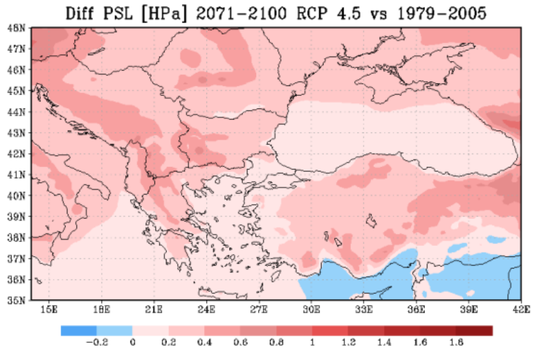

e

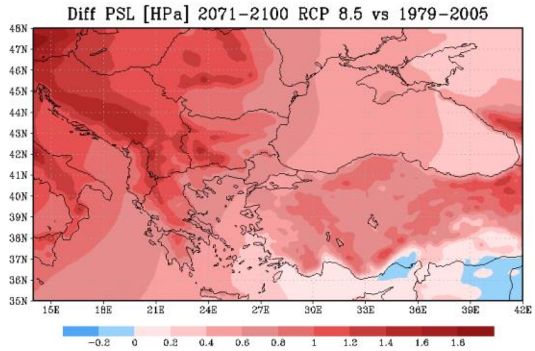

F

Fig. 5.5. Comparison of of mean sea level pressure under RCP 4.5 and RCP 8.5 scenarios for the period 2011-2040 (a,b), 2041-2070 (c,d) and 2071-2100 (e,f) and the historical period 1979-2005.

Fig. 5.5 *(b)* and *(c)* show the differences with the historical priod for the period 2041-2070. The difference is larger in the RCP8.5 scenario. During this period, under the RCP 4.5 scenario, the mean surface pressure is expected to continue increasing, with the smallest differences compared to historical period, in the southeast over Turkey and the central and eastern Black Sea, but increasing towards the northwest and reaching about 0.6 hPa - 0.7 hPa over the Balkan Peninsula. Over the Balkan Peninsula the mean surface pressure for this period under the RCP8.5 scenario is expected to increase by about 0.7 hPa - 0.8 hPa compared to the historical period.

For the last future period that we consider *(e)* and *(f)*, the mean values of the surface pressure become even higher under both scenarios, again with higher values under the RCP 8.5 scenario. Over the Mediterranean and Black Sea, the mean surface pressure is expected to be higher by about 0.2 hPa - 0.4 hPa compared to the historical period, and over the Balkan Peninsula by about 0.4 hPa - 0.6 hPa. In the RCP8.5 scenario the difference is much larger. In the eastern part of the Black Sea it is around 0.4 hPa, but increases in the west and reaches a difference of 0.8 hPa in the western part of the Black Sea compared to the historical period. In the Balkan Peninsula the difference is even larger, being about 1.2 hPa in the east and south and reaching well above 1.6 hPa in the west and northwest. Overall, however, these are not significant changes compared to the historical period. The difference is higher in the RCP 8.5 scenario.

A quantitative measure is given in Table 5.3 for the whole area. It can be seen that the differences are below 1 hPa, with the most significant difference observed for the last time period under scenario RCP8.5. The red range indicates that the mean surface pressure is expected to increase over the next 100 yr under both scenarios. The brighter the color, the larger the difference compared to the historical period.

Difference from the historical period 1979-2005	**Sea level pressure BIAS [hPa]**	**Sea level pressure RMSD [hPa]**
RCP 4.5 2011-2040	**0.15**	**0.18**
RCP 4.5 2041-2070	**0.29**	**0.37**
RCP 4.5 2071-2100	**0.25**	**0.29**
RCP 8.5 2011-2040	**0.35**	**0.38**
RCP 8.5 2041-2070	**0.40**	**0.43**
RCP 8.5 2071-2100	**0.71**	**0.80**

Table 5.3. Values of the mean and standard deviation of the model results for mean sea level pressure under the two scenarios RCP 4.5 and 8.5 and the three future periods, in the 21st century, averaged over an area covering the Balkan Peninsula and the Black Sea.

5.3.2. Interannual variability of sea level pressure under the two scenarios for the period 2011-2100.

Having considered the mean characteristics for all three periods under both scenarios, we next examine how the model represents the interannual sea level pressure trend under both scenarios. For this purpose, the data from the model simulations are averaged for each year over the period 2011-2100. The result is given in Fig 5.6.

It can be seen from Fig 5.6 that the two curves are quite different. Almost identical values are given by both scenarios by 2061 and 2062. The largest difference is in 2068 and 2091. The calculated linear trend has the same direction - both trends show an increase in mean surface pressure. The rate of increase in mean surface pressure from RCP8.5 is greater than that from RCP4.5. The linear trend for RCP4.5 is 0.3 hPa/90 yr and for the RCP8.5 scenario is 0.7 hPa/90 yr.

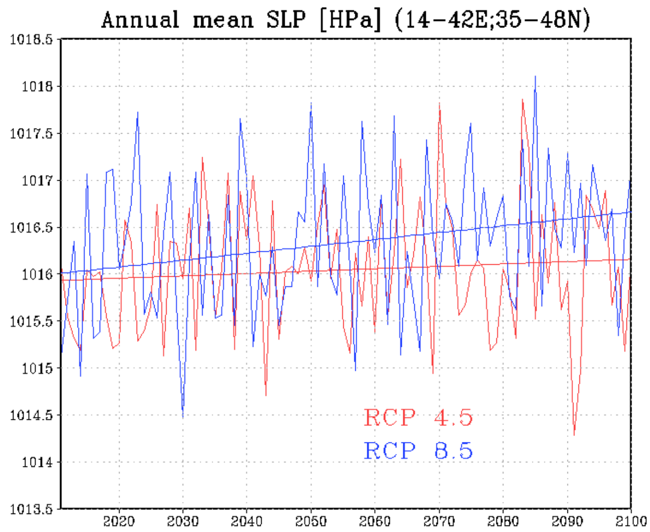

Fig. 5.6. Comparison of the interannual mean sea level pressure variability for the Balkan Peninsula and the Black Sea in model simulations for the RCP 4.5 scenario (red) and the RCP 8.5 scenario (blue) for the period 2011-2100.

5.4. Expected changes in wind speed.

Similarly to the other three meteorological elements in the previous three paragraphs, the differences between the model simulations for the two scenarios are discussed, as well as the comparison with modern climate for the wind speed at the ground.

5.4.1. Expected changes in wind speed under the two scenarios for the periods 2011-2040, 2041-2070 and 2071-2100.

Fig. 5.7. shows maps of the differences compared to the historical period and under the RCP 4.5 *(a,c,e)* and RCP 8.5 *(b,d,f)* scenarios for average surface wind speed for the three future periods - *(a)* and *(b)* for the period 2011-2041, *(c)* and *(d)* for the period 2041-2070 and *(e)* and *(f)* for the period 2071-2100.

Compared to the historical period 2011-2040 *(a)* and *(b)*, the differences are not large: under both scenarios for most of the region, the average wind speed is expected to increase slightly. Over the Balkan Peninsula and Asia Minor, the differences from the historical period are around 0.03-0.1 m/s. Higher values are observed in the western and northern Black Sea, the Sea of Azov and the northern and western Aegean Sea, where the mean wind speed is expected to increase by around 0.18 m/s under the RCP 4.5 scenario. In the RCP 8.5 scenario the picture is similar, with an increase of about 0.18 m/s in the southwestern Black Sea. In the RCP 8.5 scenario over the whole Black Sea, the increase is slightly larger than in the RCP 4.5 scenario compared to the historical period.

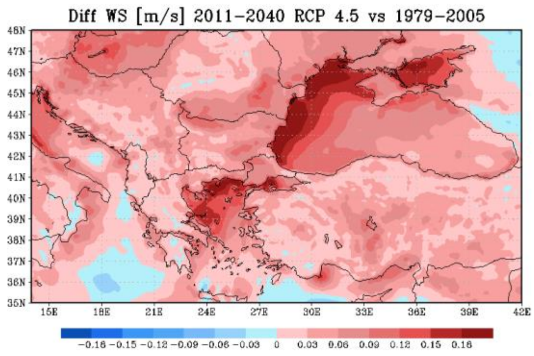

a

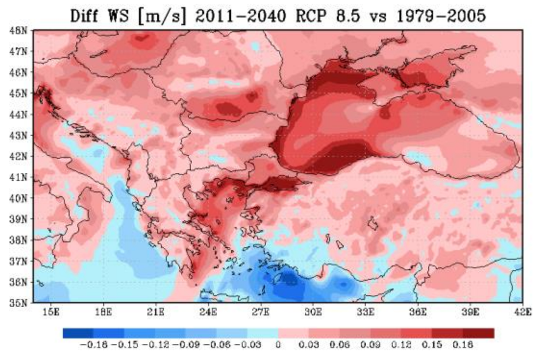

b

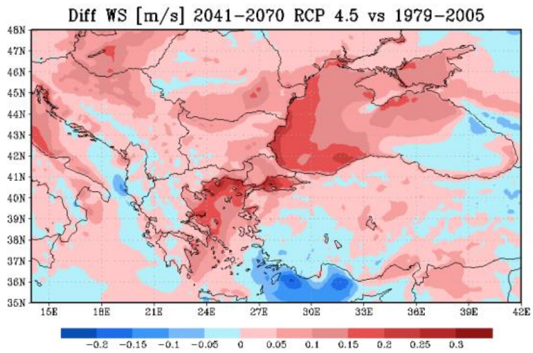

c

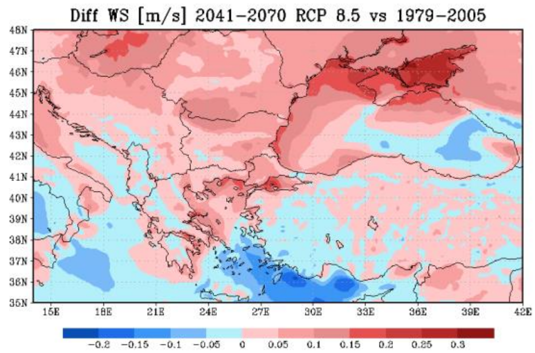

d

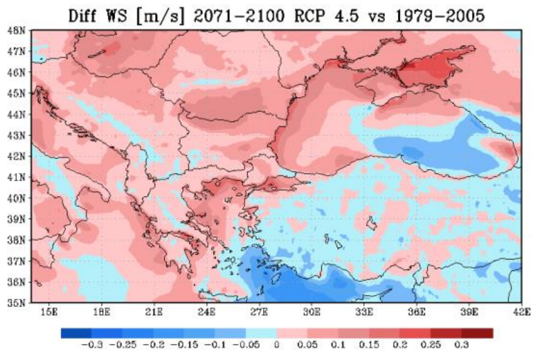

e

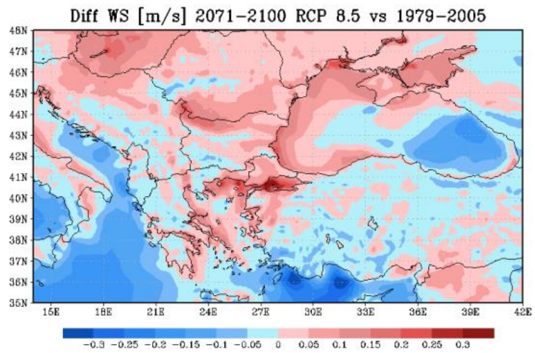

f

Fig. 5.7. Comparison of of mean surface wind speed under RCP 4.5 and RCP 8.5 scenarios for the period 2011-2040 (a,b), 2041-2070 (c,d) and 2071-2100 (e,f) and the historical period 1979-2005.

Fig. 5.7 *(c)* and *(d)* shows the difference with the historical period of the averaged wind speed, for the period 2041-2070 under the Aladin 5.2 model simulations for the RCP 4.5 scenario *(c)* and the RCP 8.5 scenario *(d)*. For both scenarios, a slight increase in mean wind speed is observed in most of the Balkan Peninsula, by about 0.05-0.1 m/s. In the RCP 4.5 scenario a slightly higher mean wind speed is observed in the south-western Black Sea and the western and northern Aegean Sea, by about 0.2 m/s. In the RCP 8.5 scenario, a similar increase is also observed in the northern Black Sea and the Sea of Azov. In the eastern Black Sea, a slight weakening of the wind is expected in both scenarios by about 0.05 m/s.

The last future time period is quite interesting for the RCP 8.5 scenario because in most places there is a weakening of the mean surface wind speed compared to the historical period, especially over the Mediterranean Sea by about 0.25 m/s in the west, down to 0.3 m/s in the east. Over the Black Sea a weakening of the mean wind speed is also observed in both scenarios, being more significant in the RCP 8.5 scenario.

For the surface wind we can conclude that no significant change is expected for the Balkan Peninsula and Black Sea region. This can be seen from Table 5.4, where the values from Fig. 5.7 are given, averaged as in the previous chapters. The red colour indicates that the average wind speed is higher compared to the historical period, and the blue colour indicates that it is lower. The brighter the color, the larger the difference relative to the historical period. It can be seen that under scenario RCP4.5, the average wind speed is initially expected to increase relative to the historical period, but decreases over time, remaining slightly above the average speed for the area considered. The RCP8.5 scenario also initially shows an increase in mean wind speed relative to the contemporary climate, but not as much as RCP4.5. However, over time, there is a more rapid weakening of the mean surface wind speed. For the latter period, the mean surface wind speed falls below the mean surface wind speed of the historical period.

Difference from the historical period 1979-2005	Mean surface wind speed BIAS [m/s]	Mean surface wind speed RMSD [m/s]
RCP 4.5 2011-2040	0.05	0.065
RCP 4.5 2041-2070	0.03	0.068
RCP 4.5 2071-2100	0.02	0.067
RCP 8.5 2011-2040	0.04	0.071
RCP 8.5 2041-2070	0.03	0.073
RCP 8.5 2071-2100	-0.007	0.077

Table 5.4. Values of the mean and standard deviation of the model results for mean surface wind speed under the two scenarios RCP 4.5 and 8.5 and the three future periods, in the 21st century, averaged over an area covering the Balkan Peninsula and the Black Sea.

From the study in Chapter 4, it is clear that the model uncertainty in representing the surface wind is on the order of 0.5 m/s, hence the changes identified by the 21st century simulations are within the error.

5.4.2. Interannual variability of surface wind under the two scenarios for the period 2011-2100.

Following the spatial averages, here we consider the inter-annual wind trend under the two scenarios for the period 2011-2100. The result is given in Fig. 5.8.

From Fig. 5.8 we can see similar values in 2038, 2045, 2090. The biggest difference is seen in 2040, where RCP4.5 gives 0.45 m/s stronger wind. Large differences are also seen in 2061, 2067, 2087, 2099. The calculated linear trend has the same direction - the mean surface wind speed decreases over time. It is interesting, however, that RCP8.5 gives higher wind values than RCP4.5 at the beginning of the period, but the values decrease much faster with time. At the end of the period RCP8.5 shows about 0.15 m/s lower wind values than RCP4.5 shows. In the RCP4.5 scenario over 90 years the linear trend is 0.02m/s, and in RCP8.5 it is 0.1m/s /90years.

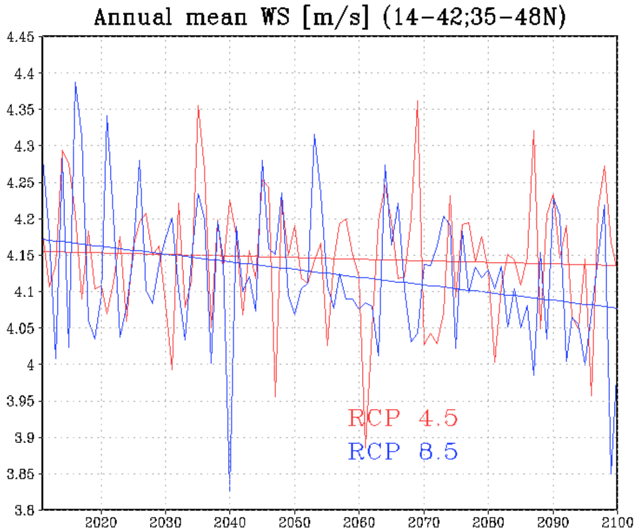

Fig. 5.8. Comparison of the interannual mean surface wind speed variability for the Balkan Peninsula and the Black Sea in model simulations for the RCP 4.5 scenario (red) and the RCP 8.5 scenario (blue) for the period 2011-2100.

6. Expected consequences of climate change in the 21st century.

6.1. Changes in winter conditions in the Black Sea region.

The Black Sea is a large deep-water basin on the boundary between the European and Asian continents, located at mid-latitudes in the continental climate zone. It is an important climatic driver for all bordering countries (Bulgaria, Romania, Ukraine, Russia, Georgia and Turkey).

Freezing of the Black Sea is regularly observed in its northern parts and near the Kerch Strait, and sometimes, when winters are very cold, it extends southwards, reaching the Romanian coast (Simonov and Altman, 1991). Since 1972, the Black Sea has experienced moderate freezing, but several extremely cold winters with high freezing events have occurred.

Our goal here, is to analyze the long-term variability of the thermal regime and severity of winters in the region in relation to freezing, based on available data for the 20th century and beyond. This may shed light on the atmospheric conditions leading to freezing and improve the predictability of such events. The results show that winter conditions were milder in the 20th century and early 21st century, but this is not directly related to freezes. Thus, ice formation can be taken as a measure of local and regional atmospheric winter conditions.

The novelty of our study is that we quantify the area covered by ice in the Black Sea using the NSIDC satellite data product, so that identification of intensive freezing events since 2006 is possible. We also obtain new information from qualitative analysis of weather conditions conducive to ice formation.

The results for daily winter ice cover for the period 2006-2021 are shown in Fig 6.1. Ice cover has occurred almost every year except the winters of 2007, 2020 and 2021 (Matov et al, 2022). Maximum ice extent was reached in February 2012, but for a relatively short period. Maximum ice cover in 2006 and 2010, for example, was smaller than in 2012, but ice formation was more stable and lasted longer.

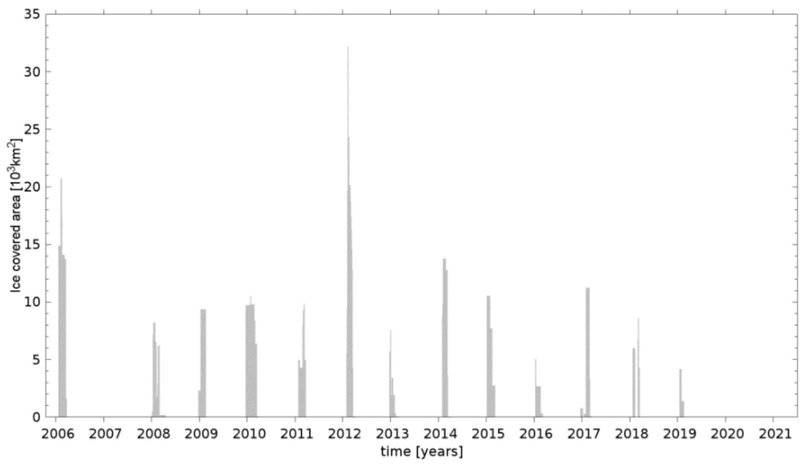

Fig. 6.1. Daily sea ice extent for the period 2006-2021 from MASIE-NH.

To make the connection between freezing and air temperature, we used data from the NOAA Global Surface Summary of the Day-GSOD (https://www.ncei.noaa.gov). In the GSOD, we used daily data from nine weather stations along the Black Sea coast-Burgas and Varna in Bulgaria, on the west coast; Odessa, Kherson, and Mariupol in the north, in Ukraine;

Batumi in Georgia on the east coast; and Istanbul, Trabzon, and Sinop on the south coast of Turkey. Data are available from 1950, but there are many gaps in the early period. The mean winter temperature was calculated for the months of January, February and March and the graphs are presented in Fig 6.2 (blue lines). As expected, the northern coastal stations (Odessa, Kherson, and Mariupol) are much colder than the southern ones (Istanbul, Sinop, and Trabzon), and the eastern one (Batumi) is similar to the southern ones as it is located on the southeastern coast. On the west coast, winter temperatures in Burgas and Varna are between southern and northern values. In general, the variations across the nine stations are very similar (except for those in Trabzon and Batumi). The calculated Pearson correlation coefficients with respect to Odessa winter temperature are as follows: 0.98 for Herson; 0.94 for Mariupol; 0.9 for Burgas; 0.93 for Varna; 0.7 for Istanbul; 0.62 for Sinop; 0.41 for Trabzon; and 0.22 for Batumi. These results suggest that winter conditions are similar over most of the basin, with the exception of the southeast. This can be explained by the prevailing northeasterly winds during winter.

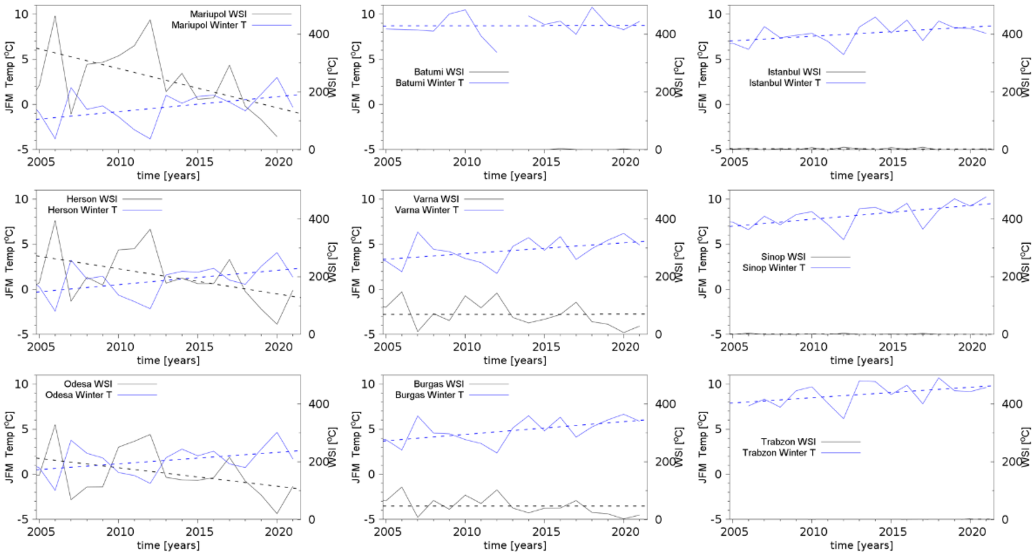

Fig 6.2. Average winter temperatures (January, February and March) in blue and WSI in black in Mariupol, Kherson, Odessa, Batumi, Varna, Burgas, Istanbul, Sinop and Trabzon for the period 2006-2021. The trends of the curves are given by a dotted line in the corresponding colour. WSI is close to zero along the southern coast in Batumi, Istanbul, Sinop and Trabzon. Periods with more than 20% missing data are not considered in this analysis.

It is interesting to note the asymmetry in the north-south and west-east directions: the mean winter temperature increases from north to south and from west to east (the latter due to westerly winds, which generally spread the influence from the sea in an easterly direction, for this latitude).

The winter intensity at the nine weather stations is presented in Fig. 6.2 using the WSI. The black lines show that Odessa, Mariupol and Kherson regularly have days with icing in winter, while in Istanbul and Sinop they are very rare. Burgas and Varna, on the west coast, are similar to the northern parts. Trabzon and Batumi practically never suffer from all-day freezing air temperatures (WSI ~ 0). There are several years with typical winter conditions for the period considered - 2006, 2012 and 2017. The last winters of 2019, 2020 and 2021 are definitely mild with very low WSI.

The positive trend in mean winter air temperature is accompanied by a negative trend in winter severity, which is particularly pronounced along the northern coast. The clear trend towards milder winters (the linear trend is shown by the dashed blue line) is consistent with the warming winter trend in the Northern Hemisphere (IPCC, 2013).

By comparing Fig. 6.1 and Fig. 6.2, it can be concluded that the relationship between freezes and WSI (winter temperature) is not direct: the trend towards milder winters is not as evident in Fig. 6.2. The freeze in the coldest years, 2006 and 2012, was actually the most intense and longest. However, in 2017, which was also very cold, the icing was moderate and less intense than in the warmer years of 2010 and 2014, so an analysis of meteorological conditions during periods of maximum sea ice extent was carried out, showing that relatively long periods below the Siberian maximum, followed by the penetration of an Arctic air mass into the periphery of an Atlantic cyclone from high latitudes, are the main meteorological conditions responsible for sea ice formation.

In Fig. 6.3 we have combined the two data sources, and we do not seek to fit the data in a single homogenized time series, as there is no overlap between the two data sources. It is clear that MASIE-NH has larger values and we believe that the reason for this is the different areas chosen for estimation. Important here is the fact that, despite the global warming trend, freezing occurs quite regularly. This is most likely due to synoptic conditions rather than seasonal averages. An interesting observation is that periods of no ice formation usually last only one year and rarely occur two years in a row. This has been the case in the recent winters of 2020 and 2021.

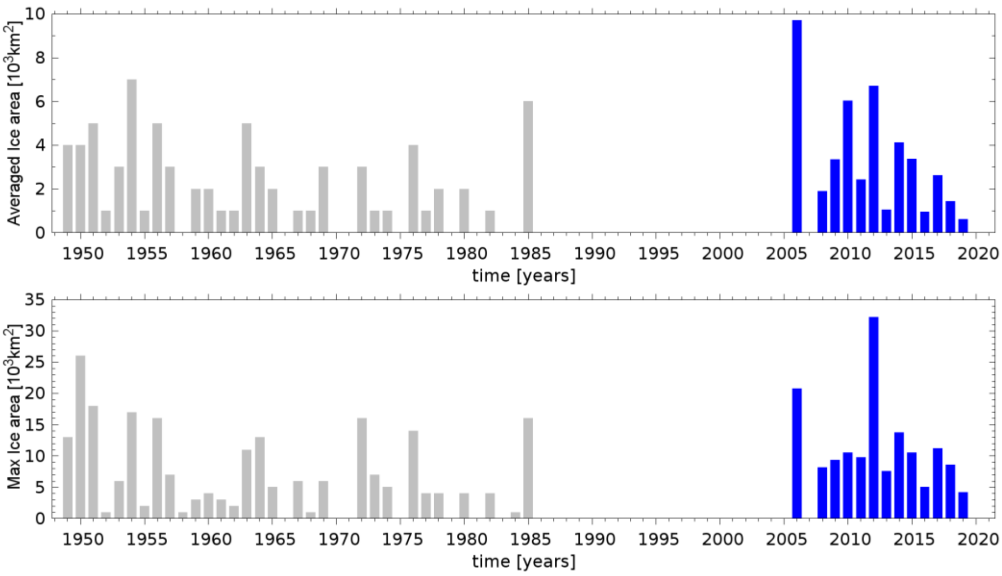

Fig. 6.3. Combined data of sea-ice extent, published in (Simonov and Altman, 1991) (grey columns) and based on MASIE-NH in the period 2006–2021 (blue columns). The upper panel presents the average area for the season December to March, and the lower shows the maximal area covered with ice in the winter season.

Regarding the mean temperature in winter, we can compare our results with those published in (Simonov and Altman, 1991). These authors give a really long record of WSI based on observations at the northern meteorological stations of Odessa, Ochakov and Horli, covering the period 1926-1985. Since the original temperature records are not available, we compared the WSI calculated from GSOD data at Odessa, Mariupol and Kherson after 1950.

The graphs in Fig. 6.4 present the WSI variations from the historical data of Simonov and Altman (1991) for the period 1926-1985; our estimated WSI from synoptic measurements in Odessa, Kherson, and Mariupol is presented after 1950, when data were available. It can be seen that the values evolve in a very similar way. Mariupol is the northernmost city and, as a result, the winter severity index is highest there. The graphs of Odessa and Kherson are similar. In 1954, winters were extremely cold in this region. The Pearson correlation coefficients of the WSI of Herson and Mariupol with respect to the WSI of Odessa are quite high - 0.97 and 0.88. In Table 5.1 we show the estimated Pearson correlation coefficient of the WSI of Odessa, Kherson and Mariupol with respect to the WSI of Simonov and Altman (1991) in the overlap period. This good correlation of the historical WSI with the Odessa WSI allows us to extend the first time series with the Odessa data. To fit the two time series, we equate the mean in the overlapping period (WSImean 220 vs. 246 °C); the standard deviations are practically equal. The missing value in the Odessa record for 1989 is replaced by the Kherson data.

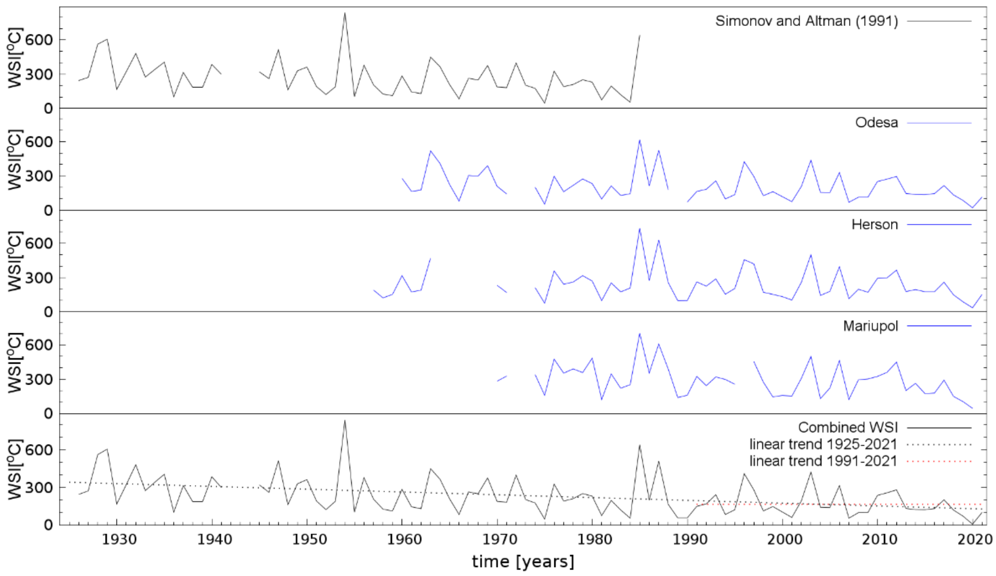

Fig 6.4 WSI of historical data for the northern Black Sea coast and WSI from Odessa, Kherson, and Mariupol from the GSOD database; the bottom panel shows the new WSI time series and the calculated linear trend with dashed line (black for the period 1926-2021 and red for the last 30 years, 1991-2021).

Pearson CC	Odesa WSI	Herson WSI	Mariupol WSI
Simonov and Altman (1991)	0.97	0.96	0.92

Table 6.1. Linear correlation coefficient between the curves in Fig. 6.4 for the overlap period 1950-1985.

Thus, we have created a new time series of the WSI that is missing only the period of World War II, 1942-1944, shown in the bottom panel of Figure 6.4. To assess the combined coherence of the WSI, we conducted a standard normal homogeneity test developed by

Alexandersson to detect potential points of change in the time series (from R: https://cran.r-project.org/web/packages/snht/snht.pdf, accessed June 11, 2022). At the 95% confidence level, the test detected one change point in 1973. We have not further modified the original time series of Simonov and Altman (1991), as there is also a gap in the record of Odessa during this period (1972-1973) from GSOD.

The most notable fact in the combined time series in Fig. 6.4 is the negative WSI trend over the period 1926-2021, estimated at ~25 °C/decade (black dashed line). We have also presented the linear trend for the last 30 years, 1991-2021 (red dashed line); the two lines almost coincide. This suggests that the trend towards warmer winters in this region since the early 20th century has not changed significantly over the nearly 100-year period.

In regard to the reported freezing event during the 20th century, there is a relation to the winter temperature, but this is not direct. Comparing Figure 10a and Figure 10b, we see that the coldest winters in 1954, 1963 and 1985 led to a large average extent of sea ice. On the contrary, the ice-free winters in 1970, 1971, 1981 and 1983 are not the warmest on record. The winter-to-winter sea ice-covered area does not necessarily follow the WSI. This again leads us to the conclusion that the mean seasonal winter temperature is not the only factor impacting the north Black Sea freezing events.

We categorize long-term winter conditions in the Black Sea region using the Winter Severity Index (WSI). The boundary values of the WSI were determined following the approach of Simonov and Altman (1991) and are given in Table 5.1 (Matov et al., 2022). According to this classification, the type of winters for the period 1926-2021 was determined. Interestingly, no truly "cold" winter conditions (e.g., WSI > 400) have been observed since 2003.

WSI Value	Winter Type
[0, 200]	Mild
[200, 400]	Moderate
[400, -]	Cold

Table 5.1. WSI threshold values used for winter classification Simonov and Altman (1991).

6.2. Changes in the intensity of seasonal centres of actin in the Black Sea region

The Balkan Peninsula and the Black Sea are located in an area which in winter is quite often influenced by the Siberian High, which invades from the northeast, and the Mediterranean Low, which influences from the south. The combination of the two can lead to quite cold winters, accompanied by precipitation and icing of the Black Sea in its northern part, as explained in the previous paragraphs. In this paragraph we will consider whether there are any changes in these centres of action over time, whether their intensity and influence on the area under consideration is changing, and whether they themselves are changing location as a result of climate change.

6.2.1. Siberian High

To quantify how the intensity of the Siberian High changes during winter, we used two measures: 1) the region-averaged pressure of 70-120E, 40-60N, and 2) the area enclosed by the 1030 hPa isobar. The data we use are from the ERA-5 reanalysis for the period 1980-2022 for the winter months (December, January, and February) only.

In Fig. 6.5, we show the interannual variability of the two selected quantitative measures of Siberian High intensity (in orange and blue). The two curves are quite similar, showing also the same positive linear trend. The conclusion is that the intensity of the Siberian maximum is strengthening, despite published reports of warming at high latitudes in the Northern Hemisphere.

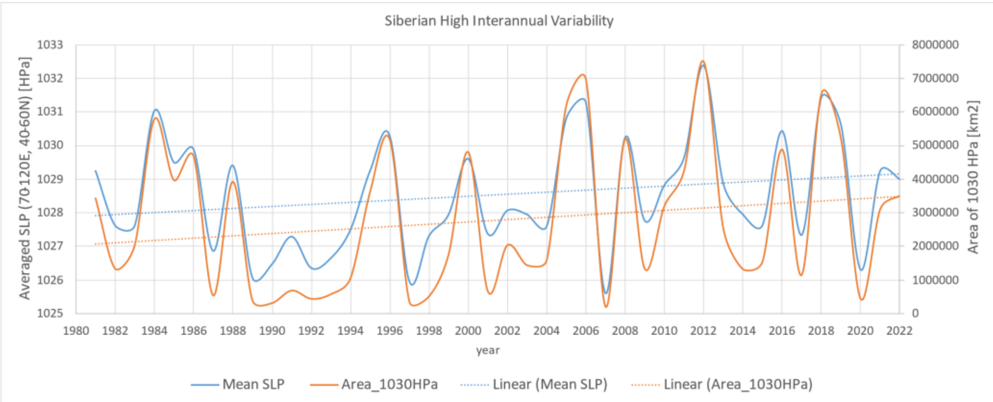

Fig 6.5 Interannual variability of the Siberian High for the winter months (December, January and February), represented by the 1030 hPa isobar in orange and the mean pressure in blue.

To project the impact of the Siberian High over the Black Sea by the end of the 21st century, we calculate the average winter pressure in the Black Sea region from Med-Cordex simulations. Higher values would be associated with a larger influence of the Siberian High. Since we do not have Siberian High data from Med-Cordex, we use those from ERA-5. Fig. 6.6 compares the mean pressure data in the Black Sea region (30-40E, 42-45N) from Med-Cordex (orange line) and from ERA-5 (blue line) for the present period. The mean pressure over the Mediterranean Sea is also given, as a measure of the other winter-active climate centre of action, the Mediterranean Low. The Pearson correlation coefficient between the averaged pressure over the Black Sea and the averaged pressure over Siberia is 0.2, while with the averaged pressure over the Mediterranean Sea it is 0.7. This indicates that the mean pressure over the Black Sea is more driven by the Mediterranean Low than the Siberian High.

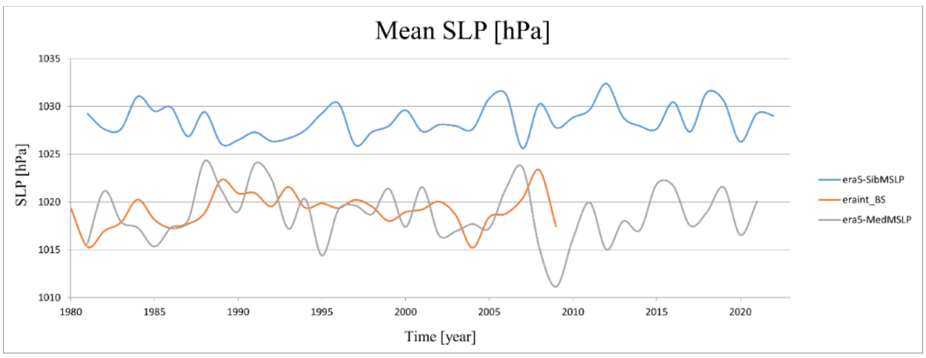

Fig 6.6 Comparison between interannual mean pressure changes for the ERA-5 region of Siberia (blue line) and the Black Sea region from Cordex data (orange line) for the period 1979-2011. The grey line represents the ERA-5 mean pressure for the Mediterranean depression.

Fig. 6.7 shows the interannual variability of the mean pressure in the Black Sea region using the Med-Cordex data (orange colour), the historical period simulated with Aladin5.2 (blue colour), as well as a projection under the RCP4.5 by the end of the century (grey colour) and RCP8.5 by the end of the century (yellow colour) scenarios. The linear trend of each of the curves is given by the corresponding line colours. The curves for the historical period coincide in some places, but differ quite a lot in others. The linear correlation coefficient between them is 0.4. The linear trend for both curves is positive, i.e. both Aladin5.2 and reanalysis show that the mean pressure for the period 1979-2005 has increased. As for the future period until the end of the century (2011-2100), the two curves for the two scenarios give quite different results, but the linear trend is positive for both scenarios, and this is more pronounced for RCP8.5. This is consistent with the results in Chapter 5 that mean sea level pressure is expected to increase by the end of the century.

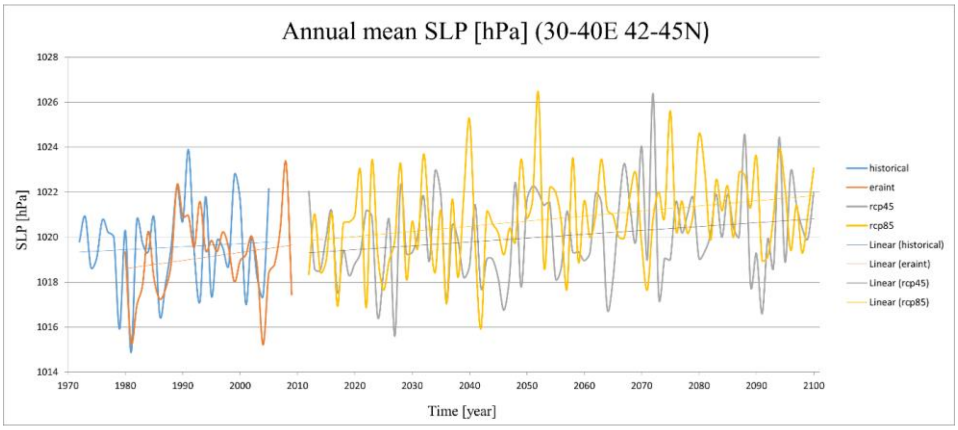

Fig 6.7. Interannual variability of mean sea level pressure for the Black Sea region for the present-day climate under ERA-Interim (orange colour) and ALADIN5.2 (blue colour) reanalysis and for the future period 2011-2100 under RCP4.5 (grey colour) and RCP8.5 (orange colour) scenarios. The linear trends of the growth curves are also given with the corresponding colours.

6.2.2. Mediterranean Low

As in the previous paragraph, in Fig. 6.7 we compare the mean pressure between the ERA-5 (orange line) and Med-Cordex (grey line) data, only this time for the Mediterranean region (0-26E, 37-41N). Here we see that the two lines are almost identical, and the correlation between them is 0.99. This is not surprising since the ECMWF atmospheric reanalysis was used as boundary conditions in the Aladin 5.2 simulations

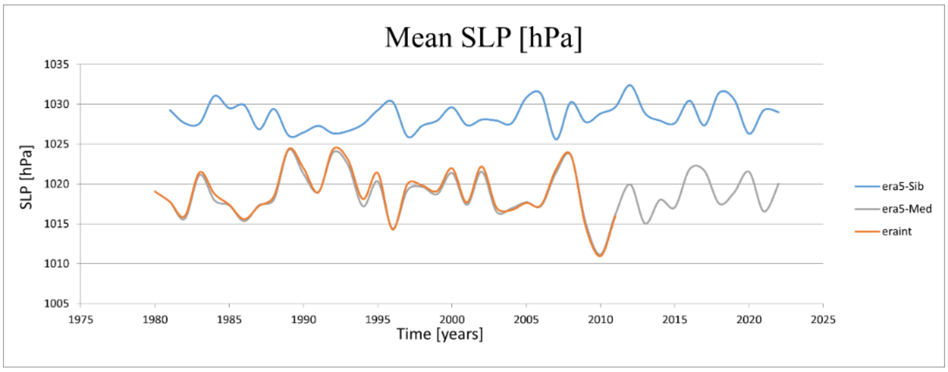

Fig 6.7. Comparison between interannual mean pressure variability for the Mediterranean region by ERA-5 (orange line) and Cordex (grey line) for the period 1979-2011. The blue line represents the ERA-5 mean pressure for the Siberian maximum.

In the next step, the goal is to make a projection of the Mediterranean Low. In Fig. 6.8, the interannual variability of the mean pressure in the Mediterranean region is given using Med-Cordex data (orange color), the historical period simulated with Aladin5.2 (blue color), the RCP4.5 scenario simulation until the end of the century (gray color) and the RCP8.5 simulation until the end of the century (yellow color). The linear trend of each of the curves is given by the corresponding line colours. Again, the two scenarios give different curves as a result, but the trends under both scenarios show a weakening of the Mediterranean Low, which is consistent with the results in Chapter 5 that mean surface pressure is expected to increase by the end of the century. It is interesting to note that the trend for the 21st century is opposite to that in the historical period.

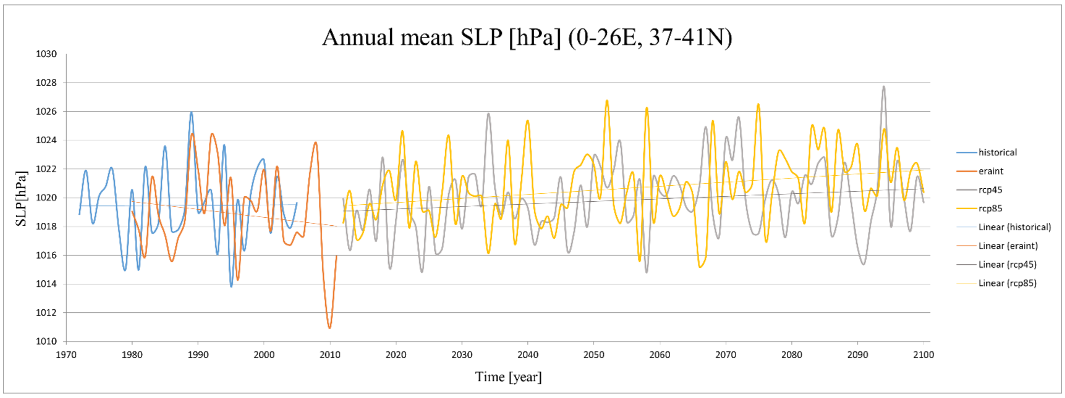

Fig 6.8. Interannual variability of mean sea level pressure for the Mediterranean region for the historical period under the Cordex data (orange colour) and ALADIN5.2 (blue colour) and for the future period 2011-2100 under the RCP4.5 (grey colour) and RCP8.5 (orange colour) scenarios. The linear trends of the growth curves are also given with the corresponding colours.

6.3. Changes in the frequency of stormy wind events

Many of the studies of future climate in the 21st century mention that extreme events - intense rains, storms, etc. - are expected to increase. In this paragraph, we analyze for the future period (2011-2100) the frequency of surface winds of different speeds. The aim is to identify whether there is a redistribution in wind strength. For each year over the Balkan Peninsula-Black Sea region, the percentage of points with wind speed values in 5 intervals is calculated:

(<5), (5-10), (10-15), (15-20) and (>20) m/s for each year. For this purpose, we cannot use the monthly data we have presented so far. The data used are three hourly, and for simplicity the projection of one of the RCP4.5 scenarios for the period 2011-2100 is taken.

Most interesting is the figure for wind speeds above 20 m/s (Fig 6.9), where the interannual variability of the percentage of points with surface wind speed values higher than 20 m/s is presented. The frequency of these winds is generally very low, but in the period 979-2006 it decreases (negative linear trend), while in the projection to the end of the 21st century it increases (positive linear trend). Despite the small number, the increase is nearly twice, which is significant.

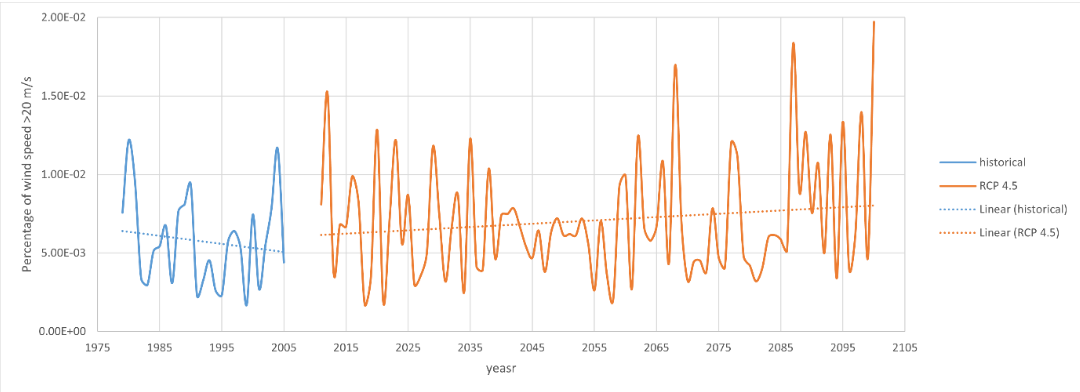

Fig 6.9. Interannual variability of the percentage of points with wind speed values above 20 m/s for the Black Sea and Balkan Peninsula region from ALADIN5.2 simulations for the historical period 1979-2005 (blue line) and the future period 2011-2100 (orange line). The linear trends for the two periods are given with the corresponding colours.

7. Conclusion

This thesis aims to obtain inferences on the expected climate changes concerning temperature, precipitation, sea level pressure and surface winds for the Black Sea and Balkan Peninsula region in the 21st century using the output of simulations with the regional climate model Aladin 5.2 for two of the RCP scenarios (4.5 and 8.5) defined in AR5. These scenarios are the starting point for all climate change research until at least 2020, with the first considered to be a moderate scenario and the second a pessimistic scenario. The data on which the estimates are based are the averaged temperature, precipitation, sea level pressure and surface wind for the Balkan Peninsula and the Black Sea for the period 1979-2005, which characterises the present-day climate, and for the period 2011-2100, which are the climate projections from the model. The results were processed and visualized with the Grid Analysis and Display System (GrADS).

As a first step in the analysis, the error of the model used is assessed, i.e. how accurately it simulates the current climate of the Balkan Peninsula and the Black Sea region in terms of temperature, precipitation, pressure and wind. Data from the ECMWF ERA-Interim meteorological analysis were used for the comparison. The results of the comparison show that for the Balkan Peninsula and Black Sea region, the model underestimates the temperature over the coast by about 1-2 degrees, while over the sea the temperature is overestimated by the model by about 1 degree. The error is smallest in winter and largest in spring and summer, with the overall BIAS being negative. As for precipitation, for the Balkan Peninsula and the Black Sea the model has an overall positive BIAS and an error of about 200 mm/y. The analysis by season shows an overestimation by the model for all seasons, with the error again being smallest in winter and largest in summer. The pressure differences are not large. The analysis shows that the model underestimates the pressure by about 1 hPa, with the error being about 2 times larger in the cold season (winter and spring) than in the summer season. Regarding wind, for the Black Sea and Balkan Peninsula region, the model has an overall positive BIAS and an error of about 0.17 m/s. Generally speaking, the simulated wind is overestimated in the Mediterranean and the Black Sea, but underestimated in most of the Aegean.

Comparison of the time series from model simulations and reanalysis of the area-averaged Black Sea and Balkan Peninsula temperature, precipitation, pressure and wind reveals a general similarity and similarity, but also the presence of periods with significant differences. The trend in temperature, both in the reanalysis and in the model, shows a significant increase, the increase in the model being slightly more significant, although the values are slightly underestimated. As for precipitation, again both trends are positive. The pressure trend in the model is towards a slight decrease, which is explained by the warming trend, while there is very little trend in the meteorological reanalysis. For the surface wind, both the model and the reanalysis give a decreasing trend with similar values.

The next step was to examine the expected changes under the two scenarios RCP4.5 and RCP8.5 separately for three future time periods (2011-2040, 2041-2070 and 2071-2100) in terms of annual mean surface temperature, precipitation, surface pressure and wind speed for the Black Sea and Balkan Peninsula region. Both scenarios show an increasing trend in mean annual temperature, surface pressure and precipitation over the next 100 years, with the increase being more significant for each successive period and for the RCP8.5 scenario relative to 4.5, respectively. The linear trend in temperature is estimated to be 2.2 ^{0}C/90 years y and 4 ^{0}C/90 years over the whole period for RCP8.5. As for precipitation, the linear trend by the end of the century is estimated to be 36.5 mm/day over 90 years for RCP4.5 and 76 mm/day over

90 years for RCP8.5. The surface pressure is estimated to be 0.2 hPa/90 years for RCP4.5 and 0.6 hPa/90 years for the whole period for RCP8.5. The surface wind trends indicate that the wind will weaken, with the linear surface wind trend estimated at -0.01 m/s/90 years for RCP4.5 and 0.1 m/s/90 years for RCP8.5. In the second scenario RCP8.5, temperature, precipitation and pressure increase more and faster, while wind weakens more and faster than in scenario RCP4.5.

Following the analysis of the four meteorological elements, we analyse the consequences of climate change for the Black Sea region and the Balkan Peninsula by examining winter conditions and ice cover in the Black Sea from 2050 to the present, changes in the centers of influence for the present and future climate - Siberian High and Mediterranean Law and the expected change in winds with speeds in the ranges (<5), (5-10), (10-15), (15-20) and (>20) m/s for the present and future climate, the periods being the same as in the analysis of temperature, precipitation, pressure and wind.

The analysis of the Black Sea freezing shows that despite the positive trend of global warming, freezing occurs quite regularly in the northern part of the sea. The analysis of meteorological conditions during periods of maximum sea ice extent shows that relatively long periods below the Siberian High, followed by the penetration of an Arctic air mass into the periphery of a high-latitude Atlantic cyclone, are the main meteorological phenomena responsible for ice formation in the Black Sea. The WSI trend is negative, which is normal with the course of global warming, and has been estimated at ~25 °C/decade for the period 1926-2021.

To see how the intensity of the Siberian High and the Mediterranean Low varies, we use both Cordex and ERA-5 data, since Cordex gives a better estimate for the Mediterranean Low and ERA-5 for the Siberian High. In this analysis, we conclude that the mean pressure over the Black Sea is more similar to the pressure over the Mediterranean (correlation 0.7) than the pressure defining the Siberian High (correlation 0.2). For both centers of action, the results show a strengthening of intensity for the modern climate, which is rather strange for the Siberian High, since it is logical that the opposite is happening due to global warming. For the future climate by the end of the century, the model estimates a strengthening of the Siberian High and a weakening of the Mediterranean Low.

As for winds in the intervals (<5) (5-10) (10-15) (15-20) (>20) m/s, we have only used the RCP4.5 scenario. The change in wind speed is not large, but what is interesting here is that the strongest helicities above 20 m/s have been decreasing in the historical period, while an increase in the frequency of these winds is observed for the future period. The number is quite small, but the model shows a significant increase.

8. Contributions of the thesis

- The expected changes in surface temperature, precipitation, sea level pressure and wind speed for the 21st century are systematized for the 2011-2040, 2041-2070, 2071-2100 tridecadal period for the Balkan Peninsula-Black Sea region under RCP4.5 and RCP8.5 scenarios.
- For the first time, the area and duration of Black Sea freezings since 2006 have been estimated from satellite observations; these results have been combined with published data for the 20th century, and the classification of winter severity has been updated using the Winter Severity Index.
- Freezings in the northern Black Sea have been found to be associated with specific synoptic conditions, not necessarily associated with low winter temperatures.
- The influence of the seasonal centers of action Siberian High and Mediterranean Low on the winter conditions in the Black Sea region is described, and the influence of the Mediterranean Low is found to be significant.
- It is found that under the RCP4.5 scenario the Mediterranean centre of action decreases in intensity by the end of the 21st century (winter pressure in the Mediterranean shows an increasing trend).
- The RCP4.5 scenario finds that the frequency of storm wind events increases by the end of the 21st century.

Part of the results in this thesis were used by the World Bank in the compilation of the National Disaster Risk Profile for Bulgaria in Chapter 4 Climate Change and Disaster Risk.

8. Publications and participation in events

- Matov M., 2019, “Climate projections for 21th Century of ground pressure and wind on the Balkan peninsula based on CORDEX project data”, Proceedings of the Second PhD Conference, 20^{th} February, Sofia, pp. 183-217 (in Bulgarian)
- Matov M., Peneva E., Georgieva G., Black sea freezing and winter severity: Relation to the temperature, Proceeding of 1^{st} International Conference on Environmental Protection and Disaster RISKs – Part One, 2020, pages:134-143
- Mirna Matov, Elisaveta Peneva, Vasko Galabov, Black Sea freezing and relation to the winter conditions in 2006-2021, Atmosphere, 2022, 13(6), 974; https://doi.org/10.3390/atmos13060974 (Q2)
- Elisaveta Peneva, Mirna Matov and Milen Tsekov, “Mediterranean Influence on the Precipitation Regime over Balkan Peninsula in the period 1901-2021 (submitted)

- Participation in the Second Doctoral Conference, Sofia University "St. Kliment Ohridski", Sofia, 2019.
- Participation in the international conference "Copernicus Marine Service General Assembly", Brussels, Belgium. At the conference I participated with a poster on "Observed freezing on the Black Sea coast and relation to the air temperature variations", 2019.
- Participation in the training seminar "Physics and Chemistry of the Earth, Atmosphere and Ocean", Varshets, 2019.
- Participation in Open Day 2019 in the Faculty of Physics with experiments and demonstrations on atmospheric pressure, wind and clouds.
- National finalist in the FameLab Bulgaria 2019 competition, held within the Sofia Science Festival and organized by the British Council. FameLab is one of the largest science communication competitions in the world.
- Participation in "Introduction to fundamental principles of science communication to diverse audiences" training organised by Science made simple, London, Cardiff and Bristol, UK, 2020.
- Participation in the international conference "EGU General Assembly 2020", with a paper on "Climate feedbacks in the Black Sea region".
- Participation in a training seminar on "Environmental Protection of the Black Sea Coast", 2020.
- Participation in “Summer School on Effective HPC for Climate and Weather”, 2020.
- Participation in the scientific conference "1st International conference on ENVIROnmental protection and disadter RISKs (EnviroRISKs 2020)".

- Participation in the second national workshop of the Copernicus programme on "Black Sea freezing in 2006-2020 as seen by the satellites", 2020
- Participation in the FirstThe National Forum on Contemporary Space Research (NAFSKI) on "Black Sea freezing in 2006-2020 and relation to winter temperature", 2020
- Participation in the training seminar "Physics and Chemistry of the Earth, Atmosphere and Ocean", Pchelin, 2020.
- Participation in training course "How to design and develop climate services", 2021.
- Participation in summer school "First Summer School on Space Research, Technology and Applications", Rozhen, 2021.
- Participation in the 32nd Lake Atanasovo Conservation Camp as a lecturer on "Climate Projections in the Black Sea and Balkan Peninsula Region", 2021.
- Participation in the training seminar "Physics and Chemistry of the Earth, Atmosphere and Ocean", Banya, 2021.
- Participation in summer school "Second Summer School on Space Research, Technology and Applications", Rozhen, 2022.
- Participation in the National Scientific Program "Environmental Protection and Risk Reduction from Adverse Events and Natural Disasters"
- Participation in the project " Popularization of the scientific and educational activities of astronomers, meteorologists and geophysicists in Bulgaria and applicable high technologies in these natural sciences". The project is aimed at presenting the scientific and educational activities of the Departments of Astronomy and Meteorology and Geophysics to key audiences of potential students

References

1. Allen, R. J., & Kovilakam, M. (2017). The Role of Natural Climate Variability in Recent Tropical Expansion. *Journal of Climate*, *30*(16), 6329–6350. https://www.jstor.org/stable/26388540
2. Befort, D.J., S. Wild, T. Kruschke, U. Ulbrich, and G.C. Leckebusch, 2016: Different long-term trends of extra-tropical cyclones and windstorms in ERA-20C and NOAA-20CR reanalyses. Atmospheric Science Letters, 17, 586–595, doi: 10.1002/asl.694.
3. Davis, N., & Birner, T. (2017). On the Discrepancies in Tropical Belt Expansion between Reanalyses and Climate Models and among Tropical Belt Width Metrics, *Journal of Climate*, *30*(4), 1211-1231.
4. Dunn, R.J.H. et al., 2012: HadISD: A Quality Controlled global synoptic report database for selected variables at long-term stations from 1973–2011. Climate of the Past, 8(5), 1649–1679, doi: 10.5194/cp-8-1649-2012.
5. Eyring, V. et al., 2016: Overview of the Coupled Model Intercomparison Project Phase 6 (CMIP6) experimental design and organization. Geoscientific Model Development, 9(5), 1937–1958, doi: 10.5194/gmd-9-1937-2016.
6. Grise, K. M., Davis, S. M., Staten, P. W., & Adam, O. (2018). Regional and Seasonal Characteristics of the Recent Expansion of the Tropics, *Journal of Climate*, *31*(17), 6839-6856.
7. IPCC, 2000: Special Report on Emissions Scenarios. A Special Report of Working Group III of the Intergovernmental Panel on Climate Change [Nakićenović, N. and R. Swart (eds.)]. Cambridge University Press, Cambridge, United Kingdom and New York, NY, USA, 570 pp., www.ipcc.ch/report/emissions-scenarios.
8. IPCC, 2021: *Climate Change 2021: The Physical Science Basis. Contribution of Working Group I to the Sixth Assessment Report of the Intergovernmental Panel on Climate Change*[Masson-Delmotte, V., P. Zhai, A. Pirani, S.L. Connors, C. Péan, S. Berger, N. Caud, Y. Chen, L. Goldfarb, M.I. Gomis, M. Huang, K. Leitzell, E. Lonnoy, J.B.R. Matthews, T.K. Maycock, T. Waterfield, O. Yelekçi, R. Yu, and B. Zhou (eds.)]. Cambridge University Press, Cambridge, United Kingdom and New York, NY, USA, In press, doi:10.1017/9781009157896.
9. IPCC. AR5 Climate Change 2013: The Physical Science Basis. In *Contribution of Working Group I to the Fifth Assessment Report of the Intergovernmental Panel on Climate Change;* Stocker, T.F., Qin, D., Plattner, G.-K., Tignor, M., Allen, S.K., Boschung, J., Nauels, A., Xia, Y., Bex, V., Midgley, P.M., Eds.; Cambridge University Press: Cambridge, UK; New York, NY, USA, 2013; 1535p.
10. Kryidin, L.N. Seasonal and interannual changes in ice coverage and position of the ice edge in the Black and Azov Seas in connection with the peculiarities of atmospheric circulation. *Trudy GOIN* **1964**, *76*, 7–79. (In Russian)
11. Kushner P.J., Held I.M., Delworth T.L., J. Clim. 14 (2001) 2238.
12. Lund, M.T. et al., 2020: A continued role of short-lived climate forcers under the Shared Socioeconomic Pathways. Earth System Dynamics, 11(4), 977–993, doi: 10.5194/esd-11-977-2020.
13. Matov, M.; Peneva, E.; Galabov, V. Black Sea Freezing and Relation to the Winter Conditions in 2006–2021. *Atmosphere* **2022**, *13*, 974. https://doi.org/10.3390/atmos13060974
14. Rao, S. et al., 2017: Future air pollution in the Shared Socio-economic Pathways. Global Environmental Change, 42, 346–358, doi: 10.1016/j.gloenvcha.2016.05.012.
15. Reichler T., Changes in the Atmospheric Circulation as Indicator of Climate Change. In Trevor M. Letcher, editor: Climate Change: Observed impacts on Planet Earth, The Netherlands, 2009, pp. 145-164.
16. Simonov, A.; Altman, E. (Eds.) *Hydrometeorology and Hydrochemistry of the USSR Seas*; Gidrometeoizdat: St. Petersburg, Russia, 1991; Volume 4, p. 426. (In Russian)

17. Staten, P. W., Grise, K. M., Davis, S. M., Karnauskas, K. B., Waugh, D. W., Maycock, A. C., Fu, Q., Cook, K., Adam, O., Simpson, I. R., Allen, R. J., Rosenlof, K., Chen, G., Ummenhofer, C. C., Quan, X., Kossin, J. P., Davis, N. A., & Son, S. (2020). Tropical Widening: From Global Variations to Regional Impacts, *Bulletin of the American Meteorological Society*, *101*(6), E897-E904.
18. Staten, P.W., Lu, J., Grise, K.M. *et al.* Re-examining tropical expansion. *Nature Clim Change* **8**, 768–775 (2018)
19. Studholme, J., & Gulev, S. (2018). Concurrent changes to Hadley circulation and the meridional distribution of tropical cyclones. *Journal of Climate*, *31*(11), 4367-4389.
20. Thompson D.W.J., Solomon S., Science 296 (2002) 895
21. Thompson D.W.J., Wallace J.M., J. Clim. 13 (2000) 1000.
22. http://cmip-pcmdi.llnl.gov/cmip5/
23. http://tntcat.iiasa.ac.at:8787/RcpDb/dsd?Action=htmlpage&page=welcome
24. http://www.euro-cordex.net/
25. http://www.ipcc.ch/publications_and_data/publications_and_data_reports.shtml
26. http://www.ipcc.ch/report/ar5/wg1/
27. http://www.metoffice.gov.uk/
28. https://cds.climate.copernicus.eu
29. https://data.nodc.noaa.gov/
30. https://data.nodc.noaa.gov/cgi-bin/iso?id=gov.noaa.ncdc:C00516
31. https://www.medcordex.eu/medcordex.php